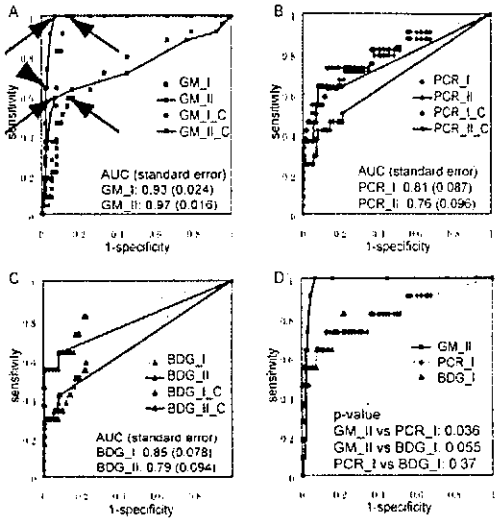

FIG. 1. (A to C) ROC curves of the GM (A), PCR (B), and BDG (C) tests for screening for IA. Both methods I and II were used. The ROC curves obtained by estimate A/B are shown in red, and those obtained by estimate C are shown in blue. The ROC curves obtained by method II are indicated by solid lines, and those obtained by method I are indicated by dotted lines. (D) Combination of ROC curves of the GM test (method II) and those of the PCR and BDG tests (method I).

reproducibility than the other two tests. The comparison of ROC curves of ELISA (method II), PCR (method I), and BDG (method I) is presented in Fig. 1D. When estimate C was applied for ROC analyses, these characteristics of the ROC curve for GM were partially obscured. In estimate C, a large decrease in sensitivity shifted the ROC curve downward and caused a significant reduction in AUC for the ELISA and BDG test, as expected. On the other hand, the ROC curve for the PCR test did not significantly change, since an expected decrease in sensitivity due to false-positive episodes in the possible IFI group is thought to be counterbalanced by a gain due to false-positive PCR results in these episodes. The ROC curves for the GM test in estimates A/B, C, and D, which is not presented but is similar to that for A/B, represent extreme cases, and the unknown "real" ROC curve might be mapped between these extremes.

Optimal cutoff value. Determination of an optimal cutoff value may be somewhat arbitrary depending on the purpose of the diagnostic test. A loss of specificity may be allowed to obtain a higher sensitivity. Based on the conventional or manufacturer-recommended cutoff values, an optical density index (O.D.I.) of 1.0, in two serial samples for GM (2, 22), i.e., 40 copies/ml for PCR and 11 pg/ml for the BDG test, all tests showed excellent specificity (0.98) in estimate A/B whereas their sensitivity was generally low (0.64, for GM, 0.45 for the PCR test, and 0.55 for the BDG test) even in estimate A/B, with further decreases as low as 0.33 for the GM test and 0.29 for the BDG test in estimate C. The current standard for ELISA (red arrowhead in Fig. 1A) seems to be inadequate. It could be reduced to 0.6 O.D.I. in method II (red arrows in Fig. 1A), or the criteria for positivity could be relaxed to those in method I while retaining the same cutoff (1.0 O.D.I.) (blue arrows), without great loss of specificity. With regard to specificity, the former may be recommended ($P = 0.0334$ by Fisher's direct test), which reflects a more leftward displacement of the ROC curve for method II. Both cutoff values represent the inflexion point of each ROC curve, around which the diagnostic efficacy is maximum for both cutoffs. The sensitivity/specificity and PPV/NPV of the GM test are 1.0/0.93 and 0.55/1.0 for a cutoff value of 0.6 O.D.I. in method II and 1.0/0.86 and 0.38/1.0 for a cutoff value of 1.0 O.D.I. in method I. Various diagnostic statistical parameters in different calculations are presented in Table 3. We may improve the diagnostic efficiency by using two or three tests in combination. In our analyses, however, we could not obtain better sensitivity by combination use of multiple tests employing much reduced cutoff values while maintaining high specificity (data not shown). This is also accompanied by significant delay of diagnosis.

Time interval between the first positive result and the antemortem diagnosis. Chronological relationships between the first positive results of different screening tests, histopathology, and diagnostic imaging are summarized in Fig. 2 and 3. For the PCR and BDG tests, the conventional cutoff was used, while the second of the first two consecutive results equal to or greater than 0.6 or 1.0 O.D.I. was plotted for ELISA. When the new reduced cutoff was used, the first positive date for GM was brought forward by a median of 10 (0 to 70, $n = 9$, mean = 24) days compared to the conventional cutoff value. Using the conventional cutoff, only one episode was identified to have a positive ELISA result before definitive treatment was started. In contrast, with the new reduced cutoff, the first positive ELISA result preceded the initiation of broad-spectrum antifungal treatment in seven IA-positive episodes (median, 31 days; range, 2 to 127 days; mean, 28 days). It became positive 51 days before a positive histopathology result (10 to 127 days; mean, 31 days).

Unfortunately, chronological comparisons between the three different assays were possible for only six episodes, in which patients had refractory leukemia and their IA tended to have a rapidly progressive course as a terminal infection (Fig. 3). In these episodes, ELISA gave positive findings earlier than (five episodes) or at the same time as (one episode) the BDG test (median, 16.5 days; range, 0 to 76 days). The PCR test was positive in 11 of 24 IA patients in estimate C. A comparison was possible in 5 of the 11 episodes, which were also positive for ELISA, but there was no significant difference in the date of the first positive result between ELISA and the PCR tests.

DISCUSSION

In this study, we compared the diagnostic potential of three different laboratory tests used to screen for IA in a prospective setting, where GM, DNA, and BDG levels in a cohort of patients at high risk for IA were measured weekly. The statistical parameters of a diagnostic test can be dramatically affected by the predetermined cutoff value, and when there is some uncertainty regarding the disease status, as in this case, they can also be influenced by the definition of the disease status. Therefore, to meaningfully compare the diagnostic potentials of these different tests, we performed an ROC analysis for each test by using the same cohort of patients with different positive result criteria (methods I and II) and various definitions of the disease status (estimates A/B, C, and D). As a

TABLE 3. Statistics for some selected thresholds

Method and threshold	Sensitivity A/B (C)	Specificity A/B (D)	PPV A/B (D)	NDV A/B (C)	Efficacy A/B (C)
Method I					
GM (O.D.I.)					
0.5	1.00 (0.88)	0.34 (0.33)	0.12 (0.11)	1.00 (0.93)	0.40 (0.43)
0.6	1.00 (0.79)	0.55 (0.54)	0.16 (0.15)	1.00 (0.93)	0.59 (0.59)
1.0	1.00 (0.58)	0.86 (0.85)	0.38 (0.34)	1.00 (0.91)	0.87 (0.81)
1.5	0.82 (0.46)	0.90 (0.89)	0.41 (0.38)	0.98 (0.90)	0.89 (0.83)
PCR (copies/ml)					
5	0.91 (0.88)	0.43 (0.41)	0.12 (0.11)	0.98 (0.95)	0.47 (0.30)
10	0.82 (0.79)	0.60 (0.55)	0.15 (0.13)	0.97 (0.94)	0.62 (0.63)
20	0.73 (0.67)	0.78 (0.75)	0.23 (0.19)	0.97 (0.92)	0.78 (0.77)
40	0.45 (0.46)	0.98 (0.93)	0.63 (0.36)	0.95 (0.90)	0.93 (0.89)
BDG (ng/ml)					
2	0.82 (0.58)	0.77 (0.76)	0.24 (0.21)	0.98 (0.91)	0.78 (0.74)
3	0.64 (0.46)	0.84 (0.82)	0.26 (0.23)	0.96 (0.89)	0.82 (0.78)
5	0.55 (0.29)	0.92 (0.92)	0.38 (0.35)	0.96 (0.87)	0.89 (0.82)
11	0.55 (0.29)	0.98 (0.97)	0.67 (0.60)	0.96 (0.88)	0.94 (0.87)
Method II					
GM (O.D.I.)					
0.5	1.00 (0.63)	0.84 (0.83)	0.35 (0.31)	1.00 (0.92)	0.85 (0.81)
0.6	1.00 (0.58)	0.93 (0.91)	0.55 (0.48)	1.00 (0.92)	0.93 (0.87)
1.0	0.64 (0.33)	0.98 (0.97)	0.70 (0.64)	0.97 (0.88)	0.95 (0.87)
1.5	0.45 (0.25)	0.98 (0.97)	0.63 (0.56)	0.95 (0.87)	0.93 (0.86)
PCR (copies/ml)					
5	0.64 (0.43)	0.87 (0.86)	0.30 (0.27)	0.96 (0.89)	0.85 (0.80)
10	0.45 (0.30)	0.94 (0.93)	0.38 (0.33)	0.95 (0.88)	0.90 (0.84)
20	0.36 (0.26)	0.98 (0.97)	0.67 (0.50)	0.95 (0.88)	0.93 (0.87)
40	0.36 (0.26)	1.00 (0.99)	1.00 (0.67)	0.95 (0.88)	0.95 (0.89)
BDG (ng/ml)					
2	0.64 (0.42)	0.91 (0.90)	0.39 (0.33)	0.97 (0.89)	0.89 (0.83)
3	0.55 (0.29)	0.95 (0.95)	0.50 (0.66)	0.96 (0.88)	0.92 (0.85)
5	0.55 (0.29)	0.98 (0.97)	0.67 (0.60)	0.96 (0.88)	0.94 (0.87)
11	0.45 (0.25)	0.99 (0.99)	0.83 (0.71)	0.95 (0.87)	0.95 (0.87)

result, the ROC curve for the GM test seemed to be better than those for the other two tests.

We previously reported that this real-time PCR for *Aspergillus* DNA was highly sensitive in vitro and with clinical samples (17): it could stably detect as few as 40 copies/ml in vitro and showed a higher sensitivity (79%) than those of the GM (58%) and BDG (67%) tests. In the present prospective analysis with consecutive patients, however, these results were not reproduced. This may be partly explained by the fact that our previous study included many retrospective samples. Furthermore, we intentionally selected IA patients and used a higher cutoff value for the GM test. Although several authors have also reported excellent sensitivity in PCR assays for IA (5, 6, 14, 34), we cannot directly compare those results with ours since there were differences in the target genes, methods of DNA extraction, starting materials, and designs of the PCR amplifications. Some form of standardization is required to make an international comparison possible. We used our real-time PCR system (GeniQ-Asper) (17) because it is most widely used in Japan. Several authors, including Loeffler et al. and Costa et al., also published excellent real-time PCR detection systems for *Aspergillus* DNA (9, 21, 26, 28), and their systems might produce superior results in the diagnosis of IA, which should be addressed in future studies.

As a diagnostic test, PCR requires more time and more complicated processing and thus costs more than the BDG and GM tests. It costs six times (15,700 yen/test) as much as the BDG and GM assays (2,700 yen/test) in Japan. A specialized laboratory as well as an expensive assay system and reagents are also required. These problems should be addressed before PCR is widely accepted as a standard screening test for IA, although it still seems to have value in making a diagnosis when a variety of clinical samples are used (20, 26, 28, 31).

The BDG test has also been widely used in Japan as a noninvasive diagnostic test for IFI. While it covers wide ranges of fungal species and may be potentially more useful as a screening test for IFI, it can cause frequent nonspecific reactions to various medical materials. Three kinds of assay systems for BDG have been developed in Japan: a chromogenic assay (FungiTec G test), β-glucan test Maruha) and a kinetic assay (β-glucan test Wako), but there is still some debate regarding their diagnostic potential. According to a sample-based analysis by Yoshida et al. (35), the chromogenic assay seems to be more sensitive (87.9 and 72.7%, respectively) than the kinetic assay but much less specific (43.3 and 75.2%, respectively) when the cutoff values recommended by the manufacturers are used. In the present study, where we used a kinetic assay, we could not obtain sufficient sensitivity even with the cutoff being maximally reduced. Furthermore, even if positive results were obtained, the positive results with the BDG test tended to occur later in the clinical course. The present result (55% sensitivity and 98% specificity) is consistent with our previous results (67% sensitivity and 84% specificity) using the chromogenic assay and also with other reports. This seems to be an inherent limitation of BDG assays

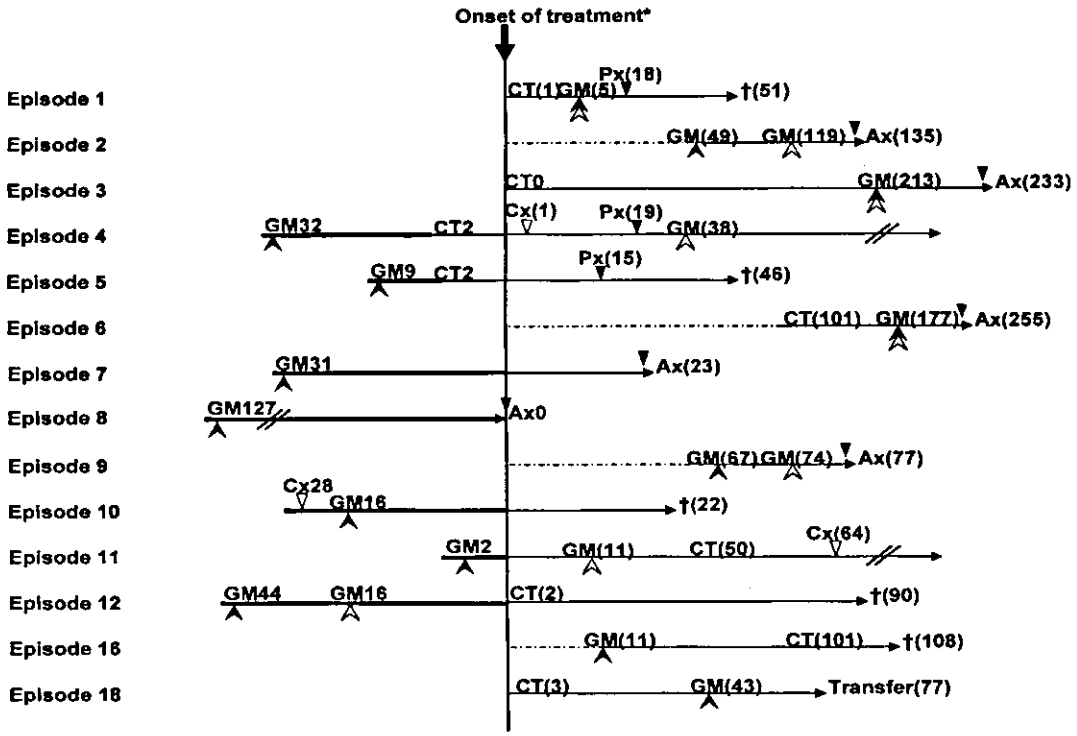

FIG. 2. Number of days from when GM assays become positive to the onset of treatment, using a threshold of 0.6 O.D.I. by method II (solid arrowheads) or 1.0 O.D.I. by method II (open arrowheads), or positive findings on CT. Open triangles indicate the date of positive culture, and solid triangles indicate when the histopathological diagnosis was made (Px, biopsy; Ax, autopsy). The values in parentheses indicate the number of days after the onset of treatment. For example, for episode 11, CT showed specific findings 50 days after the onset of treatment and the GM assay become positive 2 days before treatment. Episode numbers correspond to those in Table 2. Episodes whose GM assays did not reach the threshold are not shown. For episodes 2 and 9, a CT scan was not performed, and for episodes 7, 8, 10, 17, 19, 21, and 22, the CT findings were nonspecific and could not be used for decision-making. Each treatment was started at the discretion of the physician, taking into account various prices of clinical information, including CT findings and the results of GM assays. For Episode 8, IA was not suspected and no antifungal agent was administered. Therefore, the date of death was used instead of the date of treatment onset.

for the diagnosis of IA, although they show a very high sensitivity and specificity for candidiasis (25).

The diagnostic potential of double-sandwich ELISA for GM has been repeatedly validated in recent large-scale studies (15, 22). However, a direct comparison of the results of different studies, including ours, is not always easy and in fact can be quite difficult or impractical. Many factors can influence the apparent sensitivity and specificity and of course the PPV and NPV. Therefore, the important point is the way in which these results should be interpreted, and this depends on the objective and design of each study. From this perspective, our results are comparable to those of Maertens et al. (22) but in contrast to those of Herbrecht et al. (15). The latter addressed principally the diagnostic potential of the GM test in the presence of an unknown neutropenic fever or some respiratory signs and symptoms in cancer patients. On the other hand, in our study as well as in that of Maertens et al., the principal concern was the potential of the test in serial screenings with multiple measurements throughout the entire period of hematology care. For example, the mean numbers of measurements per episode in our study and that of Maertens et al. (8.3 and 11.2 per episode, respectively, with GM measured weekly) are significantly different from that in the study of Herbrecht et al. (5.5 per episode, with GM measured daily or weekly), consistent with the study designs. The difference becomes more prominent for proven IA episodes (17.3 and 19 versus 6.8). The differences in the mean number and timing of measurements clearly affect the apparent sensitivity and specificity of the studies. Hence, the apparent statistical values obtained by Herbrecht et al. are expected to be lower than ours and those of

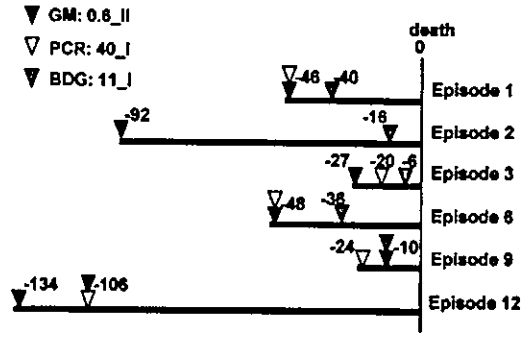

FIG. 3. Number of days before death that each test gave positive results. Solid triangles indicate the date when GM became positive, using a threshold of 0.6 O.D.I. by method II; open triangles indicate the date when PCR exceeded a cutoff value of 40 copies/ml; and shaded triangles indicate the date when the BDG test exceeded a cutoff value of 11 ng/ml, by method I. In episode 2, PCR never exceeded the cutoff value. Episode numbers correspond to those in Table 2.

Maertens et al., but they should provide a better approximation of the corresponding sample-based statistics, even though the patient population was more heterogeneous.

According to the ROC analysis of double-sandwich ELISA, the conventionally used cutoff seems to be too high: our recommendation is 0.6 O.D.I., and two consecutive positive results should be taken into consideration. With these new criteria, the GM test showed an excellent chronological profile. It gave the first positive diagnostic result in 9 of 14 GM-positive IA episodes and in 5 of 9 IA or possible IFI episodes where both CT and GM were positive. It preceded the initiation of empiric or definitive antifungal therapy in seven episodes. Using the novel criteria, positivity was ascertained a median of 10 days before conventional positivity was noted, and in six cases the GM test gave positive results only with the novel criteria. These chronological advantages were not observed with a threshold of 1.0 O.D.I. by method II: for episodes 5, 7, 8, and 10, the GM assay did not become positive; for episode 4, the GM assay exceeded the criteria 38 days after the onset of treatment; for episode 12, the GM assay gave positive results 16 days before the onset of treatment. According to the high PPV with the novel cutoff criteria (0.55 for proven or probable IA and 0.48 for proven, probable, or possible IFI) and the early timing of its positivity, we could have initiated antifungal therapy in a preemptive manner for episodes 4, 5, 7, 8, 10, 11, and 12.

Our result does not justify a discontinuation or moratorium of empiric antifungal treatment based only on a single negative result in the face of an impending threat of IA. It should be stressed that the extremely high NPVs provided here are episode-based calculations. Sample-based NPVs should be much lower, especially when patients are at high risk. We could not exclude a possibility of other IFI. Similarly, PPV does not always represent the probability of currently having IA but, rather, predicts the probability that the subject has or will have IA. In addition, while there was a sufficient number of no-IA episodes in this study to permit reliable estimations of specificity and NPV, there is much uncertainty regarding the estimations of the absolute values of sensitivity and PPV because of the small number of IA patients.

REFERENCES

1. **Andreas, S., S. Heindl, C. Wattky, K. Moller, and R. Ruchel.** 2000. Diagnosis of pulmonary aspergillosis using optical brighteners. Eur. Respir. J. 15:407–411.
2. **Ascioglu, S., J. H. Rex, B. de Pauw, J. E. Bennett, J. Bille, F. Crokaert, D. W. Denning, J. P. Donnelly, J. E. Edwards, Z. Erjavec, D. Fiere, O. Lortholary, J. Maertens, J. F. Meis, T. F. Patterson, J. Ritter, D. Selleslag, P. M. Shah, D. A. Stevens, and T. J. Walsh.** 2002. Defining opportunistic invasive fungal infections in immunocompromised patients with cancer and hematopoietic stem cell transplants: an international consensus. Clin. Infect. Dis. 34:7–14.
3. **Becker, M. J., S. de Marie, D. Willemse, H. A. Verbrugh, and I. A. Bakker-Woudenberg.** 2000. Quantitative galactomannan detection is superior to PCR in diagnosing and monitoring invasive pulmonary aspergillosis in an experimental rat model. J. Clin. Microbiol. 38:1434–1438.
4. **Bowden, R., P. Chandrasekar, M. H. White, X. Li, L. Pietrelli, M. Gurwith, J. A. van Burik, M. Laverdiere, S. Safrin, and J. R. Wingard.** 2002. A double-blind, randomized, controlled trial of amphotericin B colloidal dispersion versus amphotericin B for treatment of invasive aspergillosis in immunocompromised patients. Clin. Infect. Dis. 35:359–366.
5. **Bretagne, S., J. M. Costa, E. Bart-Delabesse, N. Dhedin, C. Rieux, and C. Cordonnier.** 1998. Comparison of serum galactomannan antigen detection and competitive polymerase chain reaction for diagnosing invasive aspergillosis. Clin. Infect. Dis. 26:1407–1412.
6. **Buchheidt, D., C. Baust, H. Skladny, J. Ritter, T. Suedhoff, M. Baldus, W. Seifarth, C. Leib-Moesch, and R. Hehlmann.** 2001. Detection of *Aspergillus* species in blood and bronchoalveolar lavage samples from immunocompromised patients by means of 2-step polymerase chain reaction: clinical results. Clin. Infect. Dis. 33:428–435.
7. **Caillot, D., O. Casasnovas, A. Bernard, J. F. Couaillier, C. Durand, B. Cuisenier, E. Solary, F. Piard, T. Petrella, A. Bonnin, G. Couillault, M. Dumas, and H. Guy.** 1997. Improved management of invasive pulmonary aspergillosis in neutropenic patients using early thoracic computed tomographic scan and surgery. J. Clin. Oncol. 15:139–147.
8. **Caillot, D., J. F. Couaillier, A. Bernard, O. Casasnovas, D. W. Denning, L. Mannone, J. Lopez, G. Couillault, F. Piard, O. Vagner, and H. Guy.** 2001. Increasing volume and changing characteristics of invasive pulmonary aspergillosis on sequential thoracic computed tomography scans in patients with neutropenia. J. Clin. Oncol. 19:253–259.
9. **Costa, C., J. M. Costa, C. Desterke, F. Botterel, C. Cordonnier, and S. Bretagne.** 2002. Real-time PCR coupled with automated DNA extraction and detection of galactomannan antigen in serum by enzyme-linked immunosorbent assay for diagnosis of invasive aspergillosis. J. Clin. Microbiol. 40:2224–2227.
10. **Denning, D. W.** 1998. Invasive aspergillosis. Clin. Infect. Dis. 26:781–803.
11. **Denning, D. W.** 1996. Therapeutic outcome in invasive aspergillosis. Clin. Infect. Dis. 23:608–615.
12. **Einsele, H., H. Hebart, G. Roller, J. Loffler, I. Rothenhofer, C. A. Muller, R. A. Bowden, J. van Burik, D. Engelhard, L. Kanz, and U. Schumacher.** 1997. Detection and identification of fungal pathogens in blood by using molecular probes. J. Clin. Microbiol. 35:1353–1360.
13. **Hanley, J. A., and B. J. McNeil.** 1983. A method of comparing the areas under receiver operating characteristic curves derived from the same cases. Radiology 148:839–843.
14. **Hebart, H., J. Loffler, C. Meisner, F. Serey, D. Schmidt, A. Bohme, H. Martin, A. Engel, D. Bunje, W. V. Kern, U. Schumacher, L. Kanz, and H. Einsele.** 2000. Early detection of aspergillus infection after allogeneic stem cell transplantation by polymerase chain reaction screening. J. Infect. Dis. 181:1713–1719.
15. **Herbrecht, R., V. Letscher-Bru, C. Oprea, B. Lioure, J. Waller, F. Campos, O. Villard, K. L. Liu, S. Natarajan-Ame, P. Lutz, P. Dufour, J. P. Bergerat, and E. Candolfi.** 2002. Aspergillus galactomannan detection in the diagnosis of invasive aspergillosis in cancer patients. J. Clin. Oncol. 20:1898–1906.
16. **Hughes, W. T., D. Armstrong, G. P. Bodey, A. E. Brown, J. E. Edwards, R. Feld, P. Pizzo, K. V. Rolston, J. L. Shenep, and L. S. Young.** 1997. 1997 guidelines for the use of antimicrobial agents in neutropenic patients with unexplained fever. Infectious Diseases Society of America. Clin. Infect. Dis. 25:551–573.
17. **Kami, M., T. Fukui, S. Ogawa, Y. Kazuyama, U. Machida, Y. Tanaka, Y. Kanda, T. Kashima, Y. Yamazaki, T. Hamaki, S. Mori, H. Akiyama, Y. Muto, H. Sakamaki, K. Osumi, S. Kimura, and H. Hirai.** 2001. Use of real-time PCR on blood samples for diagnosis of invasive aspergillosis. Clin. Infect. Dis. 33:1504–1512.
18. **Kami, M., Y. Tanaka, Y. Kanda, S. Ogawa, T. Masumoto, K. Ohtomo, T. Matsumura, T. Saito, U. Machida, T. Kashima, and H. Hirai.** 2000. Computed tomographic scan of the chest, latex agglutination test and plasma (1AE3)-beta-D-glucan assay in early diagnosis of invasive pulmonary aspergillosis: a prospective study of 215 patients. Haematologica 85:745–752.
19. **Kawamura, S., S. Maesaki, T. Noda, Y. Hirakata, K. Tomono, T. Tashiro, and S. Kohno.** 1999. Comparison between PCR and detection of antigen in sera for diagnosis of pulmonary aspergillosis. J. Clin. Microbiol. 37:218–220.
20. **Kawazu, M., Y. Kanda, S. Goyama, M. Takeshita, Y. Nannya, M. Nino, Y. Komeno, T. Nakamoto, M. Kurokawa, S. Tsujino, S. Ogawa, K. Aoki, S. Chiba, T. Motokura, N. Ohishi, and H. Hirai.** 2003. Rapid diagnosis of invasive pulmonary aspergillosis by quantitative polymerase chain reaction using bronchial lavage fluid. Am. J. Hematol. 72:27–30.
21. **Loeffler, J., N. Henke, H. Hebart, D. Schmidt, L. Hagmeyer, U. Schumacher, and H. Einsele.** 2000. Quantification of fungal DNA by using fluorescence resonance energy transfer and the light cycler system. J. Clin. Microbiol. 38:586–590.
22. **Maertens, J., J. Verhaegen, K. Lagrou, J. Van Eldere, and M. Boogaerts.** 2001. Screening for circulating galactomannan as a noninvasive diagnostic tool for invasive aspergillosis in prolonged neutropenic patients and stem cell transplantation recipients: a prospective validation. Blood 97:1604–1610.
23. **Mori, T., H. Ikemoto, M. Matsumura, M. Yoshida, K. Inada, S. Endo, A. Ito, S. Watanabe, H. Yamaguchi, M. Mitsuya, M. Kodama, T. Tani, T. Yokota, T. Kobayashi, J. Kambayashi, T. Nakamura, T. Masaoka, H. Teshima, T. Yoshinaga, S. Kohno, K. Hara, and S. Miyazaki.** 1997. Evaluation of plasma (1→3)-beta-D-glucan measurement by the kinetic turbidimetric *Limulus* test,for the clinical diagnosis of mycotic infections. Eur. J. Clin. Chem. Clin. Biochem. 35:553–560.
24. **Nakai, T., J. Uno, K. Otomo, F. Ikeda, S. Tawara, T. Goto, K. Nishimura, and M. Miyaji.** 2002. In vitro activity of FK463, a novel lipopeptide antifungal agent, against a variety of clinically important molds. Chemotherapy 48:78–81.
25. **Obayashi, T., M. Yoshida, T. Mori, H. Goto, A. Yasuoka, H. Iwasaki, H. Teshima, S. Kohno, A. Horiuchi, A. Ito, et al.** 1995. Plasma (1→3)-beta-D-glucan measurement in diagnosis of invasive deep mycosis and fungal febrile episodes. Lancet 345:17–20.

26. **Rantakokko-Jalava, K., S. Laaksonen, J. Issakainen, J. Vauras, J. Nikoskelainen, M. K. Viljanen, and J. Salonen.** 2003. Semiquantitative detection by real-time PCR of *Aspergillus fumigatus* in bronchoalveolar lavage fluids and tissue biopsy specimens from patients with invasive aspergillosis. J. Clin. Microbiol. **41**:4304–4311.
27. **Salonen, J., O. P. Lehtonen, M. R. Terasjarvi, and J. Nikoskelainen.** 2000. Aspergillus antigen in serum, urine and bronchoalveolar lavage specimens of neutropenic patients in relation to clinical outcome. Scand. J. Infect. Dis. **32**:485–490.
28. **Sanguinetti, M., B. Posteraro, L. Pagano, G. Pagliari, L. Fianchi, L. Mele, M. La Sorda, A. Franco, and G. Fadda.** 2003. Comparison of real-time PCR, conventional PCR, and galactomannan antigen detection by enzyme-linked immunosorbent assay using bronchoalveolar lavage fluid samples from hematology patients for diagnosis of invasive pulmonary aspergillosis. J. Clin. Microbiol. **41**:3922–3925.
29. **Stone, E. A., H. B. Fung, and H. L. Kirschenbaum.** 2002. Caspofungin: an echinocandin antifungal agent. Clin. Ther. **24**:351–377; discussion, 329.
30. **Stynen, D., A. Goris, J. Sarfati, and J. P. Latge.** 1995. A new sensitive sandwich enzyme-linked immunosorbent assay to detect galactofuran in patients with invasive aspergillosis. J. Clin. Microbiol. **33**:497–500.
31. **Tang, C. M., D. W. Holden, A. Aufauvre-Brown, and J. Cohen.** 1993. The detection of *Aspergillus* spp. by the polymerase chain reaction and its evaluation in bronchoalveolar lavage fluid. Am. Rev. Respir. Dis. **148**:1313–1317.
32. **Verweij, P. E., D. Stynen, A. J. Rijs, B. E. de Pauw, J. A. Hoogkamp-Korstanje, and J. F. Meis.** 1995. Sandwich enzyme-linked immunosorbent assay compared with Pastorex latex agglutination test for diagnosing invasive aspergillosis in immunocompromised patients. J. Clin. Microbiol. **33**:1912–1914.
33. **Walsh, T. J., P. Pappas, D. J. Winston, H. M. Lazarus, F. Petersen, J. Raffalli, S. Yanovich, P. Stiff, R. Greenberg, G. Donowitz, M. Schuster, A. Reboli, J. Wingard, C. Arndt, J. Reinhardt, S. Hadley, R. Finberg, M. Laverdiere, J. Perfect, G. Garber, G. Fioritoni, E. Anaissie, and J. Lee.** 2002. Voriconazole compared with liposomal amphotericin B for empirical antifungal therapy in patients with neutropenia and persistent fever. N. Engl. J. Med. **346**:225–234.
34. **Yamakami, Y., A. Hashimoto, I. Tokimatsu, and M. Nasu.** 1996. PCR detection of DNA specific for *Aspergillus* species in serum of patients with invasive aspergillosis. J. Clin. Microbiol. **34**:2464–2468.
35. **Yoshida, K., Y. Niki, H. Mitekura, M. Nakajima, H. Kawane, and T. Matsushima.** 2001. A discrepancy in the values of serum (1–3)-beta-D-glucan measured by two kits using different methods. Nippon Ishinkin Gakkai Zasshi **42**:237–242. (In Japanese.)

nature medicine

AML-1 is required for megakaryocytic maturation and lymphocytic differentiation, but not for maintenance of hematopoietic stem cells in adult hematopoiesis

Motoshi Ichikawa[1,7], Takashi Asai[1,7], Toshiki Saito[1], Go Yamamoto[1], Sachiko Seo[1], Ieharu Yamazaki[3], Tetsuya Yamagata[1,5], Kinuko Mitani[4], Shigeru Chiba[1], Seishi Ogawa[1,2], Mineo Kurokawa[1] & Hisamaru Hirai[1,6]

Embryonic development of multilineage hematopoiesis requires the precisely regulated expression of lineage-specific transcription factors, including AML-1 (encoded by *Runx1*; also known as CBFA-2 or PEBP-2αB)[1–5]. *In vitro* studies and findings in human diseases, including leukemias[6,7], myelodysplastic syndromes[8] and familial platelet disorder with predisposition to acute myeloid leukemia (AML)[9], suggest that AML-1 has a pivotal role in adult hematopoiesis. However, this role has not been fully uncovered *in vivo* because of the embryonic lethality of *Runx1* knockout in mice. Here we assess the requirement of AML-1/*Runx1* in adult hematopoiesis using an inducible gene-targeting method[10]. In the absence of AML-1, hematopoietic progenitors were fully maintained with normal myeloid cell development. However, AML-1-deficient bone marrow showed inhibition of megakaryocytic maturation, increased hematopoietic progenitor cells and defective T- and B-lymphocyte development. AML-1 is thus required for maturation of megakaryocytes and differentiation of T and B cells, but not for maintenance of hematopoietic stem cells (HSCs) in adult hematopoiesis.

Using the Cre-*lox*P sequence-specific recombination system, we generated mutant mice in which exon 5 of the *Runx1* gene could be selectively deleted by the expression of Cre recombinase (Fig. 1a). We mated mutant animals carrying deleted (*Runx1*$^{-}$) or *lox*P-flanked (*Runx1*^{fl}) alleles, and observed lethal bleeding of *Runx1*$^{-/-}$ embryos as anticipated[1,2]. In contrast, *Runx1*$^{fl/fl}$ and *Runx1*$^{fl/-}$ mice were normal (data not shown). We then bred the mutant mice with *Mx-cre*-transgenic mice to generate *Runx1*$^{fl/+}$*Mx-cre* or *Runx1*$^{fl/-}$*Mx-cre* mice. In these mice, the *Runx1*^{fl} allele could be effectively deleted in hematopoietic progenitors by using injected polyinosinic-polycytidylic acid (pIpC) to induce expression of Cre recombinase[10]. Two months after pIpC injection, genomic Southern blot analysis of *Runx1*$^{fl/-}$*Mx-cre* mice revealed that ≥90% of the bone marrow or peritoneal exudative cells, ~80% of which were morphologically normal neutrophils, had biallelic *Runx1* deletion. This indicates that *Runx1* deletion was induced in most bone marrow cells, and that most myeloid progenitors lacking AML-1 could still differentiate into mature neutrophils (Fig. 1b,c). Efficient excision of one *Runx1* allele was observed in the hematopoietic cells, including lymphocytes, of *Runx1*$^{fl/+}$*Mx-cre* mice. In contrast, only 9%, 32% and 57% of the thymocytes, splenic T cells and B cells *of Runx1*$^{fl/-}$*Mx-cre* mice, respectively, had a *Runx1*$^{-/-}$ genotype. Therefore, a large proportion of mature lymphocytes originated from lymphoid progenitor cells still expressing intact AML-1, and AML-1 deficiency should be disadvantageous to lymphocyte development.

Injection of pIpC did not cause significant differences in neutrophil counts or hemoglobin levels among the *Runx1*$^{fl/-}$*Mx-cre* (floxed) mice, *Runx1*$^{fl/+}$*Mx-cre* mice and *Runx1*$^{+/+}$*Mx-cre* (control) mice (Fig. 2a). Immediately after pIpC injection, however, platelet counts for the floxed mice declined to one-third to one-sixth of those for the control mice (Fig. 2a). Lymphocyte counts were slightly depressed after more than 4 weeks in the floxed and *Runx1*$^{fl/+}$*Mx-cre* mice. These results suggest that AML-1 is required for the maintenance of platelets and lymphocytes, but not for the sustained production of erythrocytes and neutrophils.

We next examined bone marrow cell morphology in the pIpC-treated floxed mice to determine whether thrombocytopenia results from abnormal megakaryopoiesis. The cellularity of the bone marrow and morphology of myeloid cells in the floxed mice were not remarkably altered from those of the control mice, except for a slightly elevated myeloid-erythroid ratio (2.35 ± 0.70 in floxed mice compared with 1.71 ± 0.39 in control mice; $n = 7$ (paired), $P = 0.046$ by Wilcoxon signed-rank test; Fig. 2b and data not shown). However, Wright-Giemsa staining of floxed bone marrow revealed the absence of normal megakaryocytes with abundant cytoplasm and lobulated nuclei (Fig. 2b). Instead, the floxed bone marrow contained a small number of immature megakaryocyte-like cells with occasionally separated round nuclei,

[1]Department of Hematology and Oncology and [2]Department of Regeneration Medicine for Hematopoiesis, Graduate School of Medicine, University of Tokyo, 7-3-1 Hongo, Bunkyo-ku, Tokyo, 113-8655, Japan. [3]Department of Clinical Laboratory and Pathology, Inoue Memorial Hospital, 1-16 Shindencho, Chuo-ku, Chiba, 260-0027, Japan. [4]Department of Hematology, Dokkyo University School of Medicine, 800 Kitakobayashi, Mibu, Tochigi, 321-0293, Japan. [5]Present address: Immunology section, Joslin Diabetes Center, Harvard Medical School, One Joslin Place, Boston, Massachusetts 02215, USA. [6]Deceased. [7]These authors contributed equally to this work. Correspondence should be addressed to S.O. (sogawa-tky@umin.ac.jp).

Published online 15 February 2004; doi:10.1038/nm997

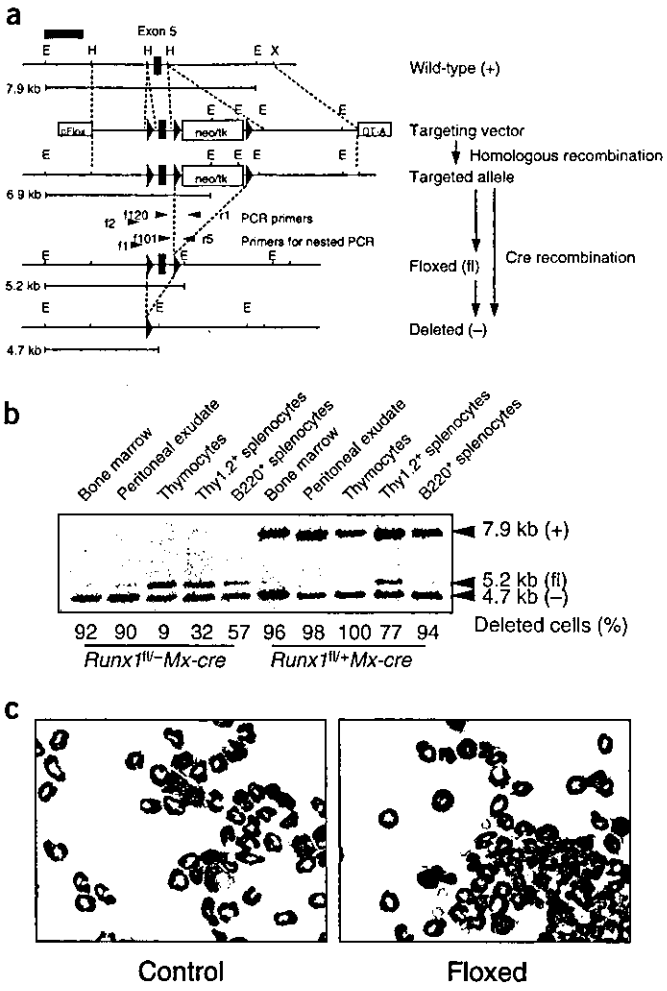

Figure 1 Inducible AML-1 knockout mice. (**a**) Schematic representation of conditional gene targeting of the *Runx1* gene. E, *Eco*RI; H, *Hin*dIII; X, *Xba*I; gray box in upper left corner, 5′ genomic probe; *neo/tk*, PGK-*neo*/HSV-thymidine kinase positive selection cassette; *DT-A*, diphtheria toxin A chain negative selection cassette. (**b**) Southern blot genotyping of cells from hematopoietic organs of mice injected with pIpC. Numbers below lanes indicate proportion of *Runx1*-deleted cells. (**c**) Wright-Giemsa-stained, cytocentrifuged specimens of peritoneal inflammatory cells genotyped in **b**.

resembling the abnormal 'micromegakaryocytes' observed in human myelodysplastic syndromes (Fig. 2b). Consistent with this observation, a substantial increase in the number of small megakaryocytes was revealed in the floxed bone marrow by acetylcholinesterase staining, which specifically detects mature and immature megakaryocytes[11] (Fig. 2b).

Given the prominent immaturity of megakaryocytes in the floxed mice, we examined the ultrastructure of the megakaryocytes (Fig. 2c). In addition to their smaller size, floxed megakaryocytes showed poorly developed demarcation membranes compared with megakaryocytes from control (*Runx1*$^{+/+}$*Mx-cre*) mice. During the maturation process, megakaryocytes acquire high DNA ploidy (>4*n*) through a cell cycle process known as endomitosis[12]. As expected from the smaller size of their nuclei, CD41$^+$ megakaryocytes from the floxed mice showed a markedly lower level of polyploidy (≤8*n*) than megakaryocytes from the control mice (modal ploidy, 16*n*), as revealed by flow cytometric measurement of DNA content. This demonstrates that AML-1 deletion also causes defective polyploidization in megakaryocytes (Fig. 2d). Although a recent report showed that AML-1 regulates the expression of megakaryocyte-specific genes in cooperation with GATA-1 (ref. 13), and although the small and immature megakaryocytes that we observed are reminiscent of those found in GATA-1 knockdown mice[14,15], the expression levels of megakaryocyte-specific transcription factors in floxed mice, including GATA-1, FOG-1 and NF-E2, remained unaffected according to RT-PCR analyses of lineage-negative (Lin$^-$) bone marrow cells (data not shown).

We subsequently conducted *in vitro* colony-forming assays to evaluate the frequency of hematopoietic progenitors. Floxed bone marrow cells formed more megakaryocytic colonies (CFU-Meg) than control bone marrow cells in semisolid media (Fig. 3a). The numbers of myeloid and mixed (myeloid and erythroid) colonies were also elevated in the floxed bone marrow. Using single-colony PCR genotyping, we detected the *Runx1*$^{-/-}$ genotype in 149 of 150 myeloid colonies, 48 of 50 erythroid colonies, 35 of 36 mixed colonies and 14 of 14 megakaryocytic colonies from pIpC-treated floxed bone marrow cells, thus excluding the possibility that those hematopoietic cells might be predominantly derived from progenitor cells still expressing intact AML-1 (data not shown). Using flow cytometry (Fig. 3b), we observed an increased number of cells in the Lin-c-Kit^{hi}CD41^{hi} fraction, which was presumed to contain CFU-Meg[16], in the floxed bone marrow. Similarly, the number of cells defined by CD34-Lin$^{-/lo}$c-Kit^{hi}Sca-1^{hi} (Fig. 3c), which represent the most immature hematopoietic progenitor cell population[17], was also elevated in the floxed bone marrow. Although development of both T and B cells from AML-1-deficient cells was impaired (Fig. 1b), the cells defined by Lin$^{-/lo}$IL-7Rα$^+$Sca-1^{lo}c-Kit^{lo}, previously reported to include common lymphocyte progenitors (CLPs)[18], were maintained in the floxed bone marrow (Fig. 3d).

Increased numbers of primitive hematopoietic progenitors, immortalized myeloid progenitor cells and arrested myeloid maturation have been observed in mice expressing the leukemic AML-1/ETO chimeric protein[19–21], which dominantly suppresses the normal function of AML-1. We observed an elevated colony-replating capacity of *Runx1*$^{-/-}$ hematopoietic cells, although replating could be repeated for only 2 months (Fig. 3e). Although AML-1-null neutrophils were morphologically normal, and freshly collected floxed bone marrow cells did not show altered apoptosis when assessed by annexin-V expression (data not shown), we detected increased apoptosis of myeloid colony-forming cells, suggesting that a certain degree of maturation arrest occurs in the myeloid lineage in the absence of AML-1 (Fig. 3f).

Because immature hematopoietic progenitor cell fractions were elevated in the floxed bone marrow, we used a competitive repopulation assay to assess their ability to reconstitute adult hematopoiesis[22]. We used isotypes of the pan-hematopoietic marker CD45 (Ly5) to distinguish the origins of the repopulating cells. Sublethally irradiated C57BL/6-Ly5.1 recipient mice (Ly5.1$^+$Ly5.2$^-$) were intravenously injected with a mixture of bone marrow cells from C57BL/6-Ly5.1/Ly5.2 F_1 competitor mice (Ly5.1$^+$Ly5.2$^+$) or floxed or control mice (Ly5.1$^-$Ly5.2$^+$) previously injected with pIpC. We then analyzed Ly5 isotypes on the repopulating cells by flow cytometry (Fig. 4a). Notably, the floxed bone marrow cells reconstituted neither peripheral T (Thy-1.2$^+$) nor B (B220$^+$) cells, whereas there were no significant differences in the mature neutrophil (Gr-1^{hi}Mac-1$^+$) and monocyte populations (Gr-1^{lo}Mac-1$^+$)[23] (Fig. 4a). The contribution to the reconstituted bone marrow was not significantly different in neutrophils (test/competitor = 0.382 ± 0.083 for floxed mice (*n* =

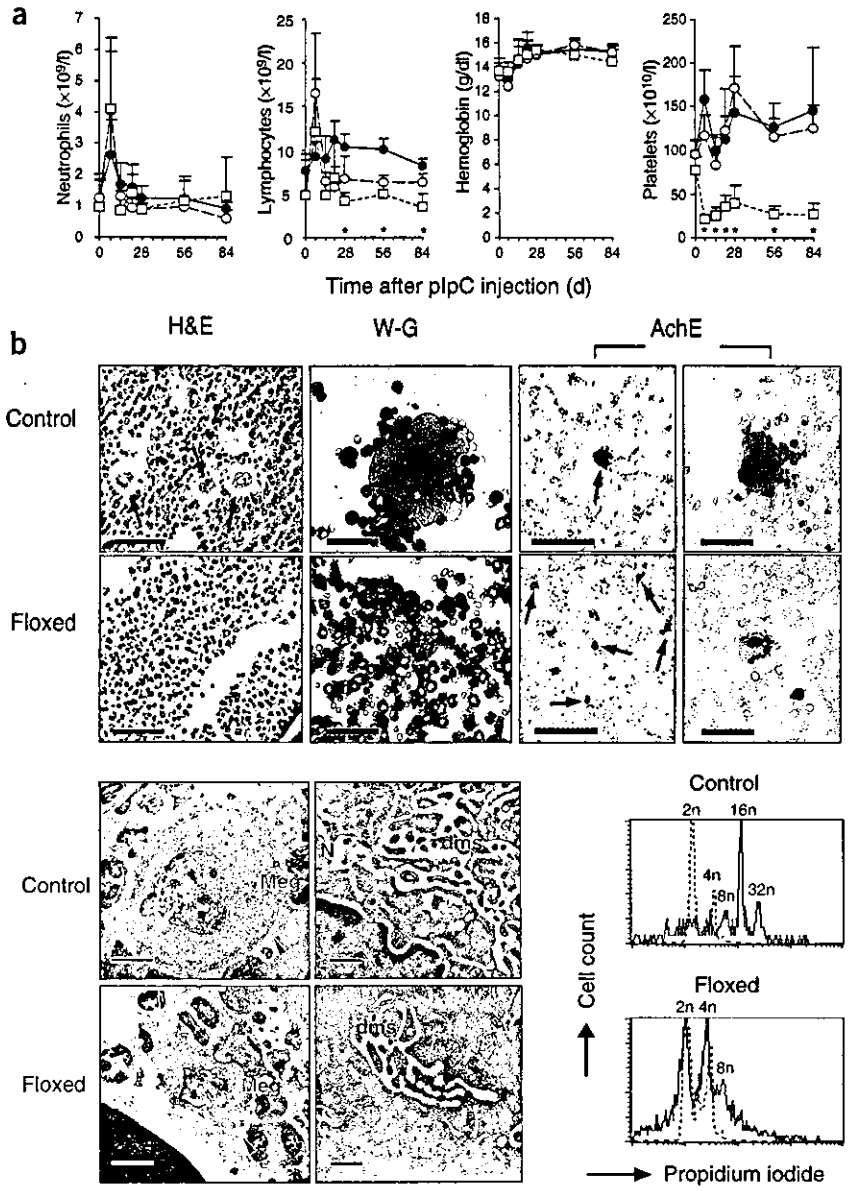

Figure 2 Thrombocytopenia and megakaryocytic maturation arrest of induced AML-1 knockout mice. (**a**) Peripheral blood cell counts of *Runx1*$^{+/+}$*Mx-cre* (control; ●), *Runx1*$^{fl/+}$*Mx-cre* (○) and *Runx1*$^{fl/-}$*Mx-cre* (floxed; □) mice injected with pIpC on days 0, 2 and 4. Results are shown as mean + s.d. (error bars) from four to seven mice. *, $P < 0.01$ for floxed compared with control mice (unequal-variance *t*-test). (**b**) Histochemical analyses of bone marrow. W-G, Wright-Giemsa; AchE, acetylcholinesterase. Arrows indicate megakaryocytes. Scale bars, 50-μm (H&E, W-G, and AchE right panel) or 250-μm (AchE left panel). (**c**) Electron micrographs of bone marrow megakaryocytes. Meg/arrowhead, megakaryocytes; dms, demarcation membranes; N, nucleus. Scale bars, 5-μm (left) or 500-nm (right). (**d**) DNA contents of CD41$^+$ bone marrow cells. – – –, CD41$^-$ fractions for 2*n* and 4*n* controls. Typical results from three experiments are shown (4–8 weeks after pIpC injection).

8), compared with 0.424 ± 0.118 for control mice ($n = 4$); $P = 0.93$ by Wilcoxon rank-sum test) or monocytes (test/competitor = 0.443 ± 0.082 for floxed mice ($n = 8$), compared with 0.940 ± 0.440 for control mice ($n = 4$); $P = 0.35$). The floxed cells also repopulated the megakaryocytic progenitors (Lin$^-$CD41$^+$; Fig. 4b). Given the inability of AML-1-deficient cells to reconstitute the T-cell lineage, we investigated thymocyte development in the absence of AML-1 by analyzing double-negative thymocytes of the recipient mice. We observed a significant block in the maturation of floxed T-cell progenitors at the transition from CD44$^+$CD25$^+$ (DN2) to CD44$^-$CD25$^+$ (DN3) (DN3/DN2 ratio of Ly5.1$^-$Ly5.2$^+$ cells = 0.025 ± 0.029 for floxed mice ($n = 5$), compared with 1.87 ± 1.51 for control mice ($n = 4$); $P < 0.05$; Fig. 4c), indicating that immature T-cell precursors had accumulated in the thymus. These findings, along with the observation that the CLP fraction was not affected in the floxed bone marrow, suggest that AML-1 is not necessary for the maintenance of CLPs, but is required in lymphoid precursors committed to T- or B-cell lineages. Consistent with this, a recent report and our experiments using *lck-Cre*-mediated, T-cell-specific AML-1-knockout mice show that the maturation of T-cell progenitors deficient in AML-1 is blocked at the DN3-DN4 transition (ref. 24 and T.A. *et al.*, unpublished data). Because *lck-Cre* expression becomes evident at the DN3 stage or later, the present study unveiled an important role of AML-1 in the DN2-DN3 transition. However, because of the insufficient contribution of the floxed cells to the B220$^+$ bone marrow fraction (test/competitor = 0.011 ± 0.012 (n = 8) compared with 0.306 ± 0.295 for control (n = 4)), we could not determine which step in B-cell development was affected by the absence of AML-1. The role of AML-1 in B-cell development might be revealed by other approaches, including the analysis of B-cell lineage-specific AML-1-knockout mice. Although lymphocyte development is substantially blocked at early stages in the absence of AML-1, the detection of AML-1-deleted T and B cells in the periphery of *Runx1*$^{fl/-}$*Mx-cre* mice (Fig. 1b) indicates that some lymphoid progenitors may still survive for a prolonged period and differentiate into mature lymphocytes.

Our data show that lack of AML-1 at the adult stage causes hematopoietic progenitor cell expansion, probably through a partial block in myeloid cell differentiation. This finding agrees with the phenotypes of previously reported mouse models of t(8;21)—carrying human leukemia, in which AML-1/ETO fusion protein is implicated in leukemogenesis through dominant-negative suppression of AML-1 function[19–21]. The loss or dominant-negative suppression of AML-1 function is also found in human myelodysplastic syndromes and familial platelet disorder with predisposition to AML[8,9], both of which are thought to be a preleukemic state. Taken as a whole, our observations suggest that the number of hematopoietic progenitor cells is negatively regulated by AML-1, and that the loss of AML-1 function triggers a preleukemic state. However, the myeloid immaturity and immortalization of bone marrow progenitors observed in AML-1/ETO mice could not be recapitulated in our *Runx1*$^{fl/-}$*Mx-cre* mice. Therefore, AML-1/ETO may not only inhibit AML-1 func-

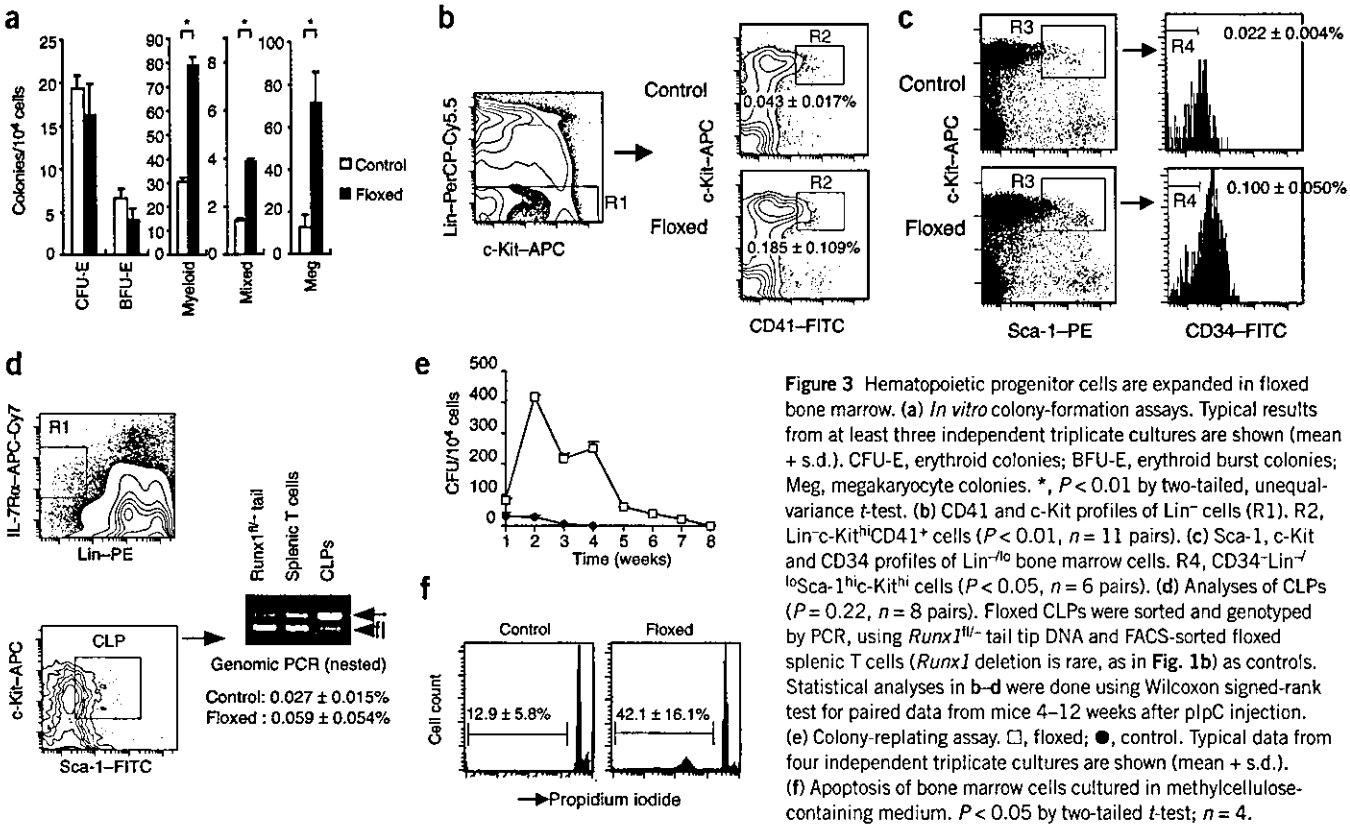

Figure 3 Hematopoietic progenitor cells are expanded in floxed bone marrow. (**a**) *In vitro* colony-formation assays. Typical results from at least three independent triplicate cultures are shown (mean + s.d.). CFU-E, erythroid colonies; BFU-E, erythroid burst colonies; Meg, megakaryocyte colonies. *, $P < 0.01$ by two-tailed, unequal-variance *t*-test. (**b**) CD41 and c-Kit profiles of Lin$^-$ cells (R1). R2, Lin$^-$c-Kit^{hi}CD41$^+$ cells ($P < 0.01$, $n = 11$ pairs). (**c**) Sca-1, c-Kit and CD34 profiles of Lin$^{-/lo}$ bone marrow cells. R4, CD34$^-$Lin$^{-/lo}$Sca-1^{hi}c-Kit^{hi} cells ($P < 0.05$, $n = 6$ pairs). (**d**) Analyses of CLPs ($P = 0.22$, $n = 8$ pairs). Floxed CLPs were sorted and genotyped by PCR, using *Runx1*$^{fl/-}$ tail tip DNA and FACS-sorted floxed splenic T cells (*Runx1* deletion is rare, as in **Fig. 1b**) as controls. Statistical analyses in **b**–**d** were done using Wilcoxon signed-rank test for paired data from mice 4–12 weeks after pIpC injection. (**e**) Colony-replating assay. □, floxed; ●, control. Typical data from four independent triplicate cultures are shown (mean + s.d.). (**f**) Apoptosis of bone marrow cells cultured in methylcellulose-containing medium. $P < 0.05$ by two-tailed *t*-test; $n = 4$.

tion, but may also have the ability to immortalize hematopoietic progenitors.

Although AML-1 is considered to be a master regulator of definitive hematopoiesis, our current study shows that AML-1 is dispensable for prolonged hematopoietic cell engraftment, as well as commitment to the myeloid lineage and at least to double-negative thymocytes in the lymphoid lineage. Our present data also indicate that AML-1 is essential for the terminal differentiation of hematopoietic progenitors of megakaryocytic and lymphocytic lineages, which establishes AML-1 as a regulator with multiple roles in the maintenance of lineage-committed cells in adult hematopoiesis. However, our results also suggest that the maintenance of HSCs and their commitment to more mature progenitors in adult hematopoiesis does not always require a transcription factor essential for hematopoietic ontogeny during embryogenesis, and can be induced by other hematopoietic genes. This is supported by a previous study

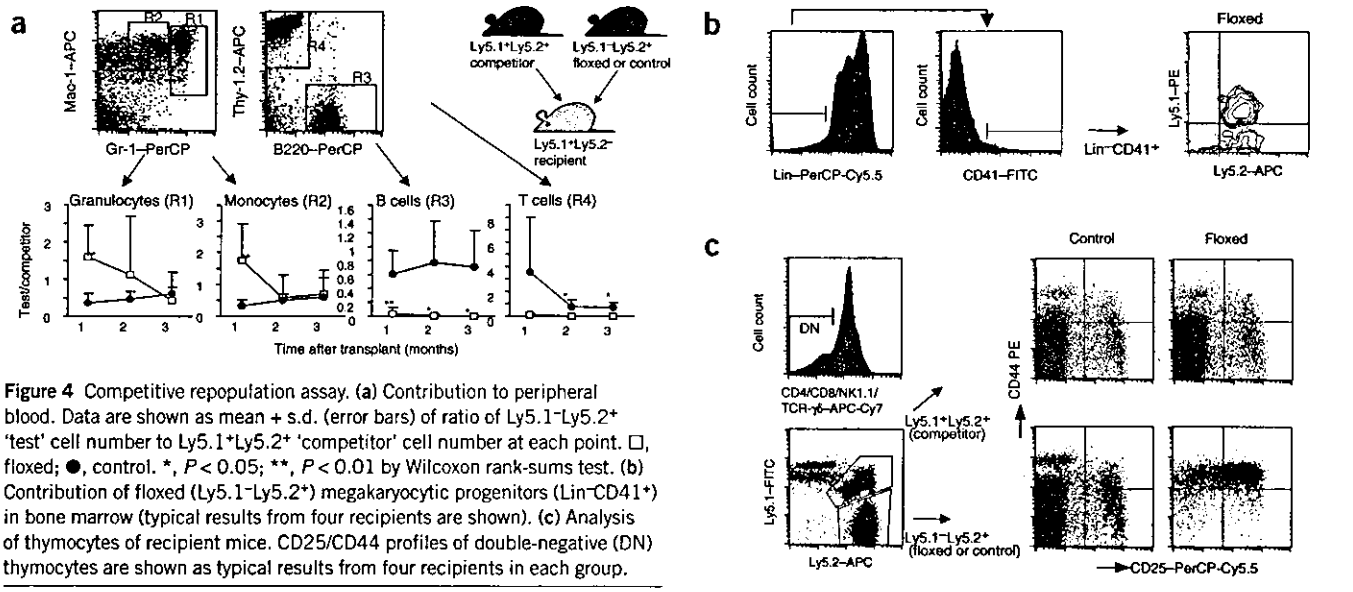

Figure 4 Competitive repopulation assay. (**a**) Contribution to peripheral blood. Data are shown as mean + s.d. (error bars) of ratio of Ly5.1$^-$Ly5.2$^+$ 'test' cell number to Ly5.1$^+$Ly5.2$^+$ 'competitor' cell number at each point. □, floxed; ●, control. *, $P < 0.05$; **, $P < 0.01$ by Wilcoxon rank-sums test. (**b**) Contribution of floxed (Ly5.1$^-$Ly5.2$^+$) megakaryocytic progenitors (Lin$^-$CD41$^+$) in bone marrow (typical results from four recipients are shown). (**c**) Analysis of thymocytes of recipient mice. CD25/CD44 profiles of double-negative (DN) thymocytes are shown as typical results from four recipients in each group.

that showed that SCL/*tal-1*, a transcription factor essential for the development of primitive hematopoiesis during the embryonic stage, is required for the proper differentiation of erythroid and megakaryocytic lineages, but not for the maintenance of HSCs in adult hematopoiesis[25]. To fully understand the intricate process of hematopoiesis, it will be necessary to determine the roles of those hematopoietic genes.

METHODS

Mice. We introduced the targeting vector (Fig. 1a) into TT2 embryonic stem cells[26], and transiently expressed Cre recombinase to generate embryonic stem cell lines carrying the *Runx1*^{fl} or *Runx1*$^{-}$ alleles. Chimeric mice raised by aggregation were crossed to the C57BL/6 background, and were mated to interferon-inducible *Mx-cre* transgenic mice[10]. *Mx-cre* expression was induced by intraperitoneally injecting 250 μg of pIpC, on three alternate days, into 4- to 8-week-old mice[10]. C57BL/6-Ly5.1 congenic and C57BL/6-Ly5.1/Ly5.2 F_1 mice were used for competitive repopulation assays. Mice were kept at the Animal Center for Biomedical Research, University of Tokyo, according to institutional guidelines.

Genotyping. For PCR genotyping, cells were lysed in a lysis buffer (0.3% Tween 20, 0.3% NP-40, and 120 μg/ml proteinase K in 1× TE buffer) at 55 °C for 1 h, followed by inactivation at 80 °C for 10 min. DNA was amplified using primers f2 (5′-ACAAAACCTAGGTGTACCAGGAGAACAAGT-3′), f120 (5′-CCCTGAAGACAGGAGAAGTTTCCA-3′) and r1 (5′-GTCTACTC-CTTGCCTCAGAAAACAAAAAC-3′) for the first PCR reaction, and nested primers f1 (5′-AAAACCTAGGTGTACCAGGAGAACAAGTC-3′), f101 (5′-TTCCAGGTCAACTCTCTCACCTCTC-3′) and r5 (5′-ATCTGAGTTGGCC TAATTTCCCTTTG-3′) for the second reaction, to detect the 280-base pair *Runx1*$^{-}$ and 220-base pair *Runx1*^{fl} products. Southern blot analyses of DNA samples digested with *Eco*RI were done according to standard protocols, using a 5′ *Eco*RI-*Bgl*II genomic probe (Fig. 1a).

Analyses of blood cells. Peripheral blood was counted using an automated hemacytometer, and leukocytes were morphologically classified to calculate neutrophil and lymphocyte counts. Mice were analyzed for bone marrow morphology 2 months after pIpC administration. For histological examination, sectioned femoral bone marrow specimens were stained with H&E, and cytocentrifuged specimens were stained with Wright-Giemsa or for acetylcholinesterase as previously described[11]. Peritoneal exudative cells were collected by washing the peritoneal cavities of mice 4 h after intraperitoneal injection of 2 ml of 2% casein in PBS. Splenocytes were labeled with antibodies to Thy-1.2 (for T cells) or B220 (for B cells), conjugated to magnetic microbeads to collect splenic lymphocytes using a MACS LS+ system (Miltenyi Biotec). The cells were checked for purity by flow cytometry (>97%; data not shown).

Ultrastructural studies. Femoral bone marrow samples prepared 4 weeks after pIpC injection as previously described[27] were examined with a JEOL 1200CX electron microscope.

Flow cytometry and cell sorting. All monoclonal antibodies and fluorochromes were purchased from BD PharMingen. To measure bone marrow progenitor cells other than CLPs, cells were stained with FITC-conjugated antibodies to CD41 or CD34, phycoerythrin (PE)-conjugated antibody to Sca-1, allophycocyanin (APC)-conjugated antibody to c-Kit, and biotin-conjugated antibodies to lineage (Lin) markers (CD3ε, CD4, CD8a, B220, Gr-1, Mac-1 and Ter119), and visualized with streptavidin-PerCP-Cy5.5. For CLP cell fractions, cells were stained with Lin-PE, Sca-1-FITC, c-Kit-APC and IL-7Rα–biotin/streptavidin-APC-Cy7. Stained samples were analyzed using either FACSCalibur or BD LSRII (BD Biosciences). For sorting CLP cells, Lin^{+} were predepleted from bone marrow cells using the MACS LD system (Miltenyi Biotec). The remaining fraction was stained for CLP as described above and sorted using a FACSVantage cell sorter. The cell sorter was calibrated to achieve >98% purity for Thy-1.2^{+} cells stained with Thy-1.2–APC. Approximately 1,000 CLP cells were genotyped by PCR. To analyze competitively repopulated cells, cells were stained with Ly5.2–FITC, Ly5.1–PE, Gr-1–biotin/streptavidin–PerCP and Mac-1–APC for myeloid cells, and with Ly5.2–FITC, Ly-5.1–PE, B220–PerCP and Thy-1.2–APC for T and B lymphocytes. Thymocytes were stained with Ly5.1–FITC, Ly5.2–APC, CD25– PerCP-Cy5.5, CD44–PE and biotin-conjugated antibodies to CD4, CD8, NK1.1 and TCR-γδ, and visualized by streptavidin–APC-Cy7 for analyzing double-negative thymocytes. Bone marrow megakaryocytic progenitors were stained with CD41–FITC, Ly-5.1–PE, Ly-5.2–APC and Lin–biotin/streptavidin-PerCP-Cy5.5. Two-color flow cytometric analysis of the DNA content of bone marrow megakaryocytes stained with CD41–FITC was performed as previously described[28].

In vitro hematopoietic colony-forming assays. For CFU-Meg, 2.5×10^4 bone marrow cells from mice 4–8 weeks after pIpC injection were cultured in 1 ml of α-MEM containing 0.8% methylcellulose, 1% BSA, 30% FBS, 100 μM 2-mercaptoethanol and 10 units of mouse thrombopoietin. For other (myeloid and erythroid) colonies, 5×10^4 cells were cultured in 1-ml of IMDM containing 0.8% methylcellulose, 1% BSA, 30% FBS, 100-μM 2-mercaptoethanol, 100-ng/ml of mouse stem cell factor, 5-ng/ml of mouse interleukin-3 and 7.5 units/ml of human erythropoietin (all growth factors were generously provided by Kirin Brewery). Colonies were counted after 3 d (for erythroid colonies), 5 d (for erythroid bursts and myeloid colonies), 7 d (for mixed colonies) or 8 d (for CFU-Meg) of culture in 5% CO_2 at 37 °C. For replating experiments, the whole myeloid and erythroid culture was pooled on day 7 and washed twice, and 1×10^4 cells were subjected to subsequent culture in the same medium. Scoring for colonies and reculturing were repeated every 7 d.

Detection of apoptotic cells. Whole myeloid and erythroid methylcellulose cultures were pooled on day 7 of culture, washed, fixed and stained with propidium iodide for analysis by flow cytometry to detect apoptotic cells (DNA content < 2*n*) as previously described[29].

Competitive repopulation assay. X-ray-irradiated (9.5-Gy, 0.3-Gy/min, unfractionated) recipient mice were intravenously injected with a mixture of 1×10^5 each of unfractionated bone marrow cells from 'test' mice (floxed or control mice, 8–12 weeks after pIpC injection) and competitor mice. Peripheral blood was analyzed monthly, and bone marrow cells and thymocytes were analyzed 3 months after transplantation by flow cytometry.

ACKNOWLEDGMENTS

We thank S. Aizawa for providing us with TT2 ES cells; T. Komori for *Runx1* genomic fragments; J. Takeda for *Mx-cre*-transgenic mice; and thank K. Kumano, A. Kunisato and other members of H.H.'s lab for critical discussion. This work was supported in part by a Grant-in-Aid for Scientific Research (KAKENHI 13307029, 15689015) from the Japan Society for the Promotion of Science, and by Health and Labour Sciences Research grants from the Ministry of Health, Labour and Welfare.

COMPETING INTERESTS STATEMENT

The authors declare that they have no competing financial interests.

Received 4 November 2003; accepted 20 January 2004
Published online at http://www.nature.com/naturemedicine/

1. Okuda, T., van Deursen, J., Hiebert, S.W., Grosveld, G. & Downing, J.R. AML1, the target of multiple chromosomal translocations in human leukemia, is essential for normal fetal liver hematopoiesis. *Cell* **84**, 321–330 (1996).
2. Wang, Q. *et al.* Disruption of the *Cbfa2* gene causes necrosis and hemorrhaging in the central nervous system and blocks definitive hematopoiesis. *Proc. Natl. Acad. Sci. USA* **93**, 3444–3449 (1996).
3. Mukouyama, Y. *et al.* The AML1 transcription factor functions to develop and maintain hematogenic precursor cells in the embryonic aorta-gonad-mesonephros region. *Dev. Biol.* **220**, 27–36 (2000).
4. Yokomizo, T. *et al.* Requirement of Runx1/AML1/PEBP2αB for the generation of haematopoietic cells from endothelial cells. *Genes Cells* **6**, 13–23 (2001).
5. North, T.E. *et al.* Runx1 expression marks long-term repopulating hematopoietic stem cells in the midgestation mouse embryo. *Immunity* **16**, 661–672 (2002).
6. Tenen, D.G., Hromas, R., Licht, J.D. & Zhang, D.E. Transcription factors, normal myeloid development, and leukemia. *Blood* **90**, 489–519 (1997).
7. Lutterbach, B. & Hiebert, S.W. Role of the transcription factor AML-1 in acute leukemia and hematopoietic differentiation. *Gene* **245**, 223–235 (2000).
8. Imai, Y. *et al.* Mutations of the AML1 gene in myelodysplastic syndrome and their functional implications in leukemogenesis. *Blood* **96**, 3154–3160 (2000).
9. Song, W.J. *et al.* Haploinsufficiency of CBFA2 causes familial thrombocytopenia with pro-

pensity to develop acute myelogenous leukaemia. *Nat. Genet.* **23**, 166–175 (1999).
10. Kuhn, R., Schwenk, F., Aguet, M. & Rajewsky, K. Inducible gene targeting in mice. *Science* **269**, 1427–1429 (1995).
11. Jackson, C.W. Cholinesterase as a possible marker for early cells of the megakaryocytic series. *Blood* **42**, 413–421 (1973).
12. Kaushansky, K. The enigmatic megakaryocyte gradually reveals its secrets. *Bioessays* **21**, 353–360 (1999).
13. Elagib, K.E. *et al.* RUNX1 and GATA-1 coexpression and cooperation in megakaryocytic differentiation. *Blood* **101**, 4333–4341 (2003).
14. Shivdasani, R.A., Fujiwara, Y., McDevitt, M.A. & Orkin, S.H. A lineage-selective knockout establishes the critical role of transcription factor GATA-1 in megakaryocyte growth and platelet development. *EMBO J.* **16**, 3965–3973 (1997).
15. Takahashi, S. *et al.* Role of GATA-1 in proliferation and differentiation of definitive erythroid and megakaryocytic cells *in vivo*. *Blood* **92**, 434–442 (1998).
16. Hodohara, K., Fujii, N., Yamamoto, N. & Kaushansky, K. Stromal cell-derived factor-1 (SDF-1) acts together with thrombopoietin to enhance the development of megakaryocytic progenitor cells (CFU-MK). *Blood* **95**, 769–775 (2000).
17. Osawa, M., Hanada, K., Hamada, H. & Nakauchi, H. Long-term lymphohematopoietic reconstitution by a single CD34-low/negative hematopoietic stem cell. *Science* **273**, 242–245 (1996).
18. Kondo, M., Weissman, I.L. & Akashi, K. Identification of clonogenic common lymphoid progenitors in mouse bone marrow. *Cell* **91**, 661–672 (1997).
19. Rhoades, K.L. *et al.* Analysis of the role of AML1-ETO in leukemogenesis, using an inducible transgenic mouse model. *Blood* **96**, 2108–2115 (2000).
20. Higuchi, M. *et al.* Expression of a conditional AML1-ETO oncogene bypasses embryonic lethality and establishes a murine model of human t(8;21) acute myeloid leukemia. *Cancer Cell* **1**, 63–74 (2002).
21. de Guzman, C.G. *et al.* Hematopoietic stem cell expansion and distinct myeloid developmental abnormalities in a murine model of the AML1-ETO translocation. *Mol. Cell. Biol.* **22**, 5506–5517 (2002).
22. Szilvassy, S.J., Humphries, R.K., Lansdorp, P.M., Eaves, A.C. & Eaves, C.J. Quantitative assay for totipotent reconstituting hematopoietic stem cells by a competitive repopulation strategy. *Proc. Natl. Acad. Sci. USA* **87**, 8736–8740 (1990).
23. Lagasse, E. & Weissman, I.L. Flow cytometric identification of murine neutrophils and monocytes. *J. Immunol. Methods* **197**, 139–150 (1996).
24. Taniuchi, I. *et al.* Differential requirements for Runx proteins in CD4 repression and epigenetic silencing during T lymphocyte development. *Cell* **111**, 621–633 (2002).
25. Mikkola, H.K. *et al.* Haematopoietic stem cells retain long-term repopulating activity and multipotency in the absence of stem-cell leukaemia SCL/tal-1 gene. *Nature* **421**, 547–551 (2003).
26. Yagi, T. *et al.* A novel ES cell line, TT2, with high germline-differentiating potency. *Anal. Biochem.* **214**, 70–76 (1993).
27. Breton-Gorius, J., Reyes, F., Duhamel, G., Najman, A. & Gorin, N.C. Megakaryoblastic acute leukemia: identification by the ultrastructural demonstration of platelet peroxidase. *Blood* **51**, 45–60 (1978).
28. Jackson, C.W., Brown, L.K., Somerville, B.C., Lyles, S.A. & Look, A.T. Two-color flow cytometric measurement of DNA distributions of rat megakaryocytes in unfixed, unfractionated marrow cell suspensions. *Blood* **63**, 768–778 (1984).
29. Sherwood, S.W. & Schimke, R.T. Cell cycle analysis of apoptosis using flow cytometry. *Methods Cell Biol.* **46**, 77–97 (1995).

Bone Marrow Transplantation (2004) 34, 595–602
© 2004 Nature Publishing Group All rights reserved 0268-3369/04 $30.00
www.nature.com/bmt

Recovery of Vα24$^+$ NKT cells after hematopoietic stem cell transplantation

K Haraguchi[1,2,3], T Takahashi[1], K Hiruma[2], Y Kanda[1], Y Tanaka[2], S Ogawa[1], S Chiba[1], O Miura[3], H Sakamaki[2] and H Hirai[1,4]

[1]*Department of Hematology and Oncology, Graduate School of Medicine, University of Tokyo, Bunkyo-ku, Tokyo, Japan;* [2]*Hematopoietic Cell Transplantation Team, Tokyo Metropolitan Komagome Hospital, Bunkyo-ku, Tokyo, Japan; and* [3]*Department of Hematology and Oncology, Graduate School of Medicine, Tokyo Medical and Dental University, Bunkyo-ku, Tokyo, Japan*

Summary:

Human Vα24$^+$ natural killer T (NKT) cells have an invariant T-cell receptor-α chain and are activated in a CD1d-restricted manner. Vα24$^+$ NKT cells are thought to regulate immune responses and to play important roles in the induction of allograft tolerance. In this report, we analyzed the recovery of Vα24$^+$ NKT cells after hematopoietic stem cell transplantation and its correlation with graft-versus-host disease (GVHD). Patients who received a dose-reduced conditioning regimen, antithymocyte globulin- or CAMPATH-1H-containing conditioning regimen were excluded. NKT cells were reconstituted within 1 month after transplantation in peripheral blood stem cell transplantation recipients, while their numbers remained low for more than 1 year in bone marrow transplantation (BMT) recipients. The number of Vα24$^+$ NKT cells in BMT recipients with acute GVHD was lower than that in patients without acute GVHD, and both the CD4$^+$ and CD4$^-$ Vα24$^+$ NKT subsets were significantly reduced. With regard to chronic GVHD, BMT recipients with extensive GVHD had significantly fewer Vα24$^+$ NKT cells than other patients. Furthermore, the number of CD4$^+$ Vα24$^+$ NKT cells was also significantly reduced in patients with chronic extensive GVHD. Our results raise the possibility that the number of Vα24$^+$ NKT cells could be related to the development of GVHD.

Bone Marrow Transplantation (2004) **34**, 595–602. doi:10.1038/sj.bmt.1704582
Published online 9 August 2004
Keywords: NKT cells; GVHD; immune reconstitution

Immune reconstitution after hematopoietic stem cell transplantation has been studied by many researchers. Natural killer (NK) cells are reconstituted within 1 month. While the number of CD8$^+$ T cells quickly returns to the normal range, the recovery of CD4$^+$ T cells can take a year or more.[1] In recipients of peripheral blood stem cells, T-cell counts are higher than those in marrow recipients in the first year after transplantation. However, there have been no reports on natural killer T- (NKT) cell reconstitution after hematopoietic stem cell transplantation.[2]

NKT cells are a population of T cells that have NK cell markers such as NK1.1 (NKR-P1C) in mice or CD161 (NKR-P1A) in humans. Most NKT cells use an invariant T-cell receptor (TCR)-α chain (Vα14-Jα18 in mice, Vα24-Jα18 in humans) paired with Vβ8, Vβ7, or Vβ2 in mice, or with Vβ11 in humans.[3–7] Human invariant Vα24$^+$ NKT cells as well as mouse invariant Vα14$^+$ NKT cells are activated by synthetic glycolipids such as α-galactosylceramide in a CD1d-restricted manner. NKT cells produce both Th1 (such as interferon (IFN)-β or tumor necrosis factor (TNF)-α) and Th2 (such as interleukin (IL)-4, IL-5, IL-10, IL-13) cytokines. They can control immune responses to infection and some tumors.[8,9] On the other hand, it is thought that their natural physiological role is immunoregulation, such that they regulate autoimmune diseases or allograft rejection.[8,9]

Graft-versus-host disease (GVHD) is one of the most important complications of hematopoietic stem cell transplantation. It has been shown in a mouse acute GVHD model that bone marrow NK1.1$^+$ T cells can suppress GVHD.[10] It has also been reported that CD8$^+$, CD1d-independent NKT cells, can reduce GVHD in mice.[11] However, there have been no reports on whether or not invariant NKT cells can regulate GVHD.

In this report, we analyzed the recovery of human Vα24$^+$ NKT cells after hematopoietic stem cell transplantation and its correlation with GVHD.

Patients, materials, and methods

Patients and donors

The patients' characteristics are shown in Table 1. They all gave their written informed consent to participate in the study. The procedures were approved by our institutional

Correspondence: Dr K Haraguchi, Department of Hematology and Oncology, Graduate School of Medicine, University of Tokyo, 7-3-1 Hongo, Bunkyo-ku, Tokyo 113-8655, Japan.
E-mail: kyoh-tky@umin.ac.jp
[4]Hisamaru Hirai died on August 23, 2003, during the preparation of this manuscript.
Received 9 January 2004; accepted 14 April 2004
Published online 9 August 2004

Table 1 Patients' characteristics

	BMT, n=81(32)[a]	*PBSCT, n=25(7)*
Related/unrelated	14(4)/67(28)	25(7)/0
HLA full match/1 locus mismatch	63(22)/18(10)	23(5)/2(2)
Male/female	52(21)/29(11)	13(4)/12(3)
Age (years)		
Range	16–55	17–53
Median	39	33
Diagnosis		
ALL	17	9
AML	24	8
MLL	1	0
ATL	1	0
CML	16	3
MDS	12	2
MM	2	0
MPD	1	0
NHL	3	3
AA	4	0
Conditioning regimen		
TBI-containing regimen	45(19)	14(4)
No TBI regimen	36(13)	11(3)
GVHD prophylaxis		
Cyclosporine + short-term MTX	69(27)	25(7)
Tacrolimus + short-term MTX	12(5)	0
Acute GVHD		
Grade 0	15	10
Grade I	13	6
Grade II	15	2
Grade III	5	0
Grade IV	1	0
Days to the onset of acute GVHD		
Range	7–73	5–53
Median	13	14
Chronic GVHD		
No	20(13)	6(1)
Limited	11(6)	5(4)
Extensive	16(13)	2(2)
Days to the onset of chronic GVHD		
Range	60–300	110–264
Median	140	200
CMV viremia	20(2)	4
Relapse	13(7)	7(2)

ALL = acute lymphoblastic leukemia; AML = acute myelogenous leukemia; MLL = acute mixed lineage leukemia; ATL = adult T-cell leukemia; CML = chronic myelogenous leukemia; MDS = myelodysplastic disease; MM = multiple myeloma; MPD myeloproliferative disease; NHL = non-Hodgkin lymphoma; AA = aplastic anemia; MTX = methotrexate; CMV = cytomegalovirus.
[a]Numbers within parentheses indicate patients from whom blood samples we could not take during acute phase.

review board. The patients received allogeneic bone marrow transplantation (BMT) or allogeneic peripheral blood stem cell transplantation (PBSCT) at the University of Tokyo Hospital or the Tokyo Metropolitan Komagome Hospital from March 2000 to September 2003. Blood samples were obtained on days 30, 60, 90, and 120–150 in the acute phase, and from 150 to 1155 in the chronic phase after transplantation. Patients who received a dose-reduced conditioning regimen, antithymocyte globulin- or a CAMPATH-1H-containing conditioning regimen were excluded from this study. Patients who received a second transplantation were also excluded. None of the patients received T-cell-depleted grafts.

The normal range for the number of invariant NKT cells in peripheral blood was determined by examining 30 male and 30 female healthy volunteers.

Flow cytometry analysis

Mononuclear cells were separated from blood samples by density-gradient centrifugation (Lymphoprep; AXIS-SHIELD PoC AS, Oslo, Norway). Cells were stained with fluorochrome-conjugated monoclonal antibodies (anti-CD3-FITC (clone UCHT1), anti-CD4-PC5 (clone 13B8.2), anti-TCR Vα24-FITC (clone C15), and anti-TCR Vβ11-PE (clone C21) (Immunotech, Marseille, France) and analyzed by a FACSCalibur apparatus using CellQuest software following the manufacturer's protocol (Becton Dickinson, San Jose, CA, USA). Lymphocytes were gated on forward- and side-scatter plots and the percentage of each lymphocyte subset was determined. The absolute lymphocyte count was determined by a clinical blood test. Each absolute lymphocyte subset count was calculated as the absolute lymphocyte count multiplied by the percentage of the lymphocyte subset divided by 100.

Chimerism of NKT Cells

Genomic DNA was extracted from Vα24 and Vβ11 double-positive cells, which were sorted from the peripheral blood of the recipients (by FACSVantage (Becton Dickinson)) and subjected to a short tandem repeat (STR)-PCR analysis as described previously.[12] Briefly, an STR fragment (D20S471 for pts. 002, 013, and 014, and D22S684 for pt. 003) that showed different allelic polymorphism in a given donor/recipient pair was PCR amplified from extracted DNA and analyzed by an ABI PRISM 377 DNA sequencer in combination with Genescan 3.1 software (Applied Biosystems, Foster City, CA, USA), with which different polymorphic peaks were separated and quantified to evaluate chimerism. Primer sequences were 5′-FAM GGGATGCAGAAATTGCAGTA and TTTTCTCTTTGCCACTGACC for D20S471, and 5′-HEX CCCTCTCCCTCTCTTACAGG and TTCTTAGT GGGGAAGGGATC for D22S684.

Statistical analysis

A statistical analysis was performed with the nonparametric Mann–Whitney *U*-test. A *P*-value of less than 0.05 was considered significant.

Results

Frequency of Vα24+ NKT cells in healthy donors

To measure Vα24+ NKT cells, we counted double-positive cells (Figure 1a). Previous reports have shown that such

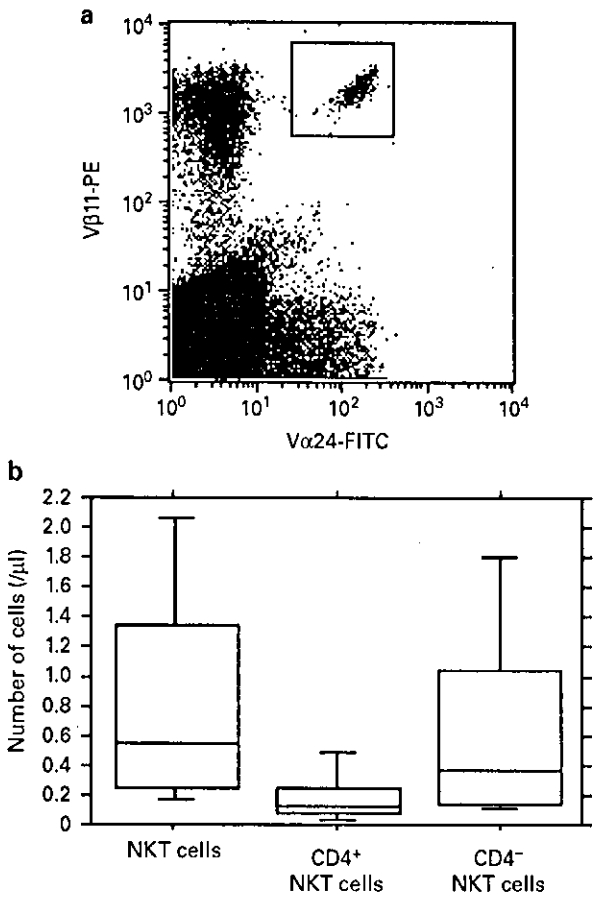

Figure 1 Frequency of Vα24+ NKT cells in healthy donors. (a) To measure Vα24+ NKT cells, we counted Vα24 and Vβ11 double-positive cells. The results of flow cytometry on a sample from a healthy donor with a Vα24+ NKT cell count of 0.543/μl are shown. Peripheral blood mononuclear cells from healthy donors (male: $n = 30$; female: $n = 30$) were stained by three-color fluorescence (Vα24-FITC/Vβ11-PE/CD4-PC5) and analyzed by flow cytometry. Lymphocytes were gated on forward- and side-scatter plots and the ratio of Vα24/Vβ11 cells for each lymphocyte subset was determined. The absolute lymphocyte count was determined by a clinical blood test. (b) Composite box plots for the numbers of NKT cells in healthy donors are shown for all Vα24+ NKT cells, CD4+ Vα24+ NKT cells, and CD4− Vα24+ NKT cells. These and all subsequent box plots show the median (horizontal line), 25th and 75th percentiles (box), and 10th and 90th percentiles (error bars). Statistical analysis was performed with the nonparametric Mann–Whitney *U*-test in all subsequent box plots.

cells have invariant TCR-α chain expression[13,14] and are CD1d dependent.[15,16]

The normal range of Vα24+ NKT cells is shown in Figure 1b. The values of the 25th, 50th, and 75th percentiles were 0.239, 0.552, and 1.345/μl, respectively. The median number as a percentage of total mononuclear cells was 0.026%, which was similar to the values in the previous reports.[16–18]

Number of Vα24+ NKT cells varied according to the graft source

There was a significant difference in the number of reconstituted NKT cells between BMT and PBSCT in the acute phase (Figure 2a) and chronic phase (data not shown). In univariate and multivariate analyses, the only variable associated with the number of NKT cells was the stem cell source (PB or BM) in the acute phase. In the chronic phase, similar results were obtained in a univariate analysis, but not in a multivariate analysis. (Variables evaluated included stem cell source (PB or BM, sibling or unrelated), diagnosis, HLA disparity, GVHD prophylaxis, with or without cytomegalovirus (CMV) viremia, GVHD, and with or without steroid treatment.) Since chronic-phase samples were collected between 150 and 1155 days after transplantation, the univariate and multivariate analyses also included time post transplant, but this was not considered as a variable. In BMT, NKT cells were not reconstituted within a year (Figure 2b). In contrast, the number of NKT cells was within the normal range at 1 month after PBSCT (Figure 2c). It was unclear as to whether the number of NKT cells in BMT patients would reach the normal range after 1 year.

We could analyze the chimerism of NKT cells in only four patients in the chronic phase (one received PBSCT and the others received BMT) by PCR-based assays of polymorphic STR markers. They all showed <10% recipient chimerism.

Number of Vα24+ NKT cells in patients with GVHD was lower than that in patients without GVHD in BMT

Since the number of NKT cells in patients who received related BMT was not significantly different from that in patients who received unrelated BMT (data not shown), we analyzed related and unrelated BMT together. The number of Vα24+ NKT cells in BMT recipients without acute GVHD was significantly higher than that in BMT recipients with acute GVHD (Figure 3a). Patients with GVHD were treated with steroids in many cases. Since lymphocytes are decreased when steroids are administered, the treatment of GVHD might reduce the number of NKT cells. However, the administration of steroids to patients with or without GVHD did not significantly affect the number of NKT cells (Figure 3b). In addition, since Vα24+ NKT cells almost universally express inflammatory lymphocyte chemokine receptors, and these receptors may cause them to be distributed at sites of inflammation,[18] they may have been removed from the blood in GVHD patients. However, there was no correlation between CMV viremia and the number of NKT cells (Figure 3c). Most of the Vα24+ NKT subsets are CD4−CD8− (double-negative: DN) and CD4+, although there is a small subset of the CD8+ phenotype in peripheral blood.[14] Since there are so few CD8+ NKT cells and since they are so similar to DN NKT cells,[14] we examined CD4+ and CD4− NKT cells. Both CD4+ and CD4− Vα24+ NKT cells were significantly reduced in patients with acute GVHD (Figure 3d,e). Since there were so few patients with grade III or IV GVHD, we could not evaluate whether or not the severity of GVHD was correlated with the number of NKT cells.

Beyond 150 days after BMT, the number of Vα24+ NKT cells in chronic extensive GVHD patients was significantly lower than that in patients who had no or limited chronic GVHD (Figure 4a). Furthermore, there were significantly fewer CD4+ Vα24+ NKT cells in chronic extensive GVHD

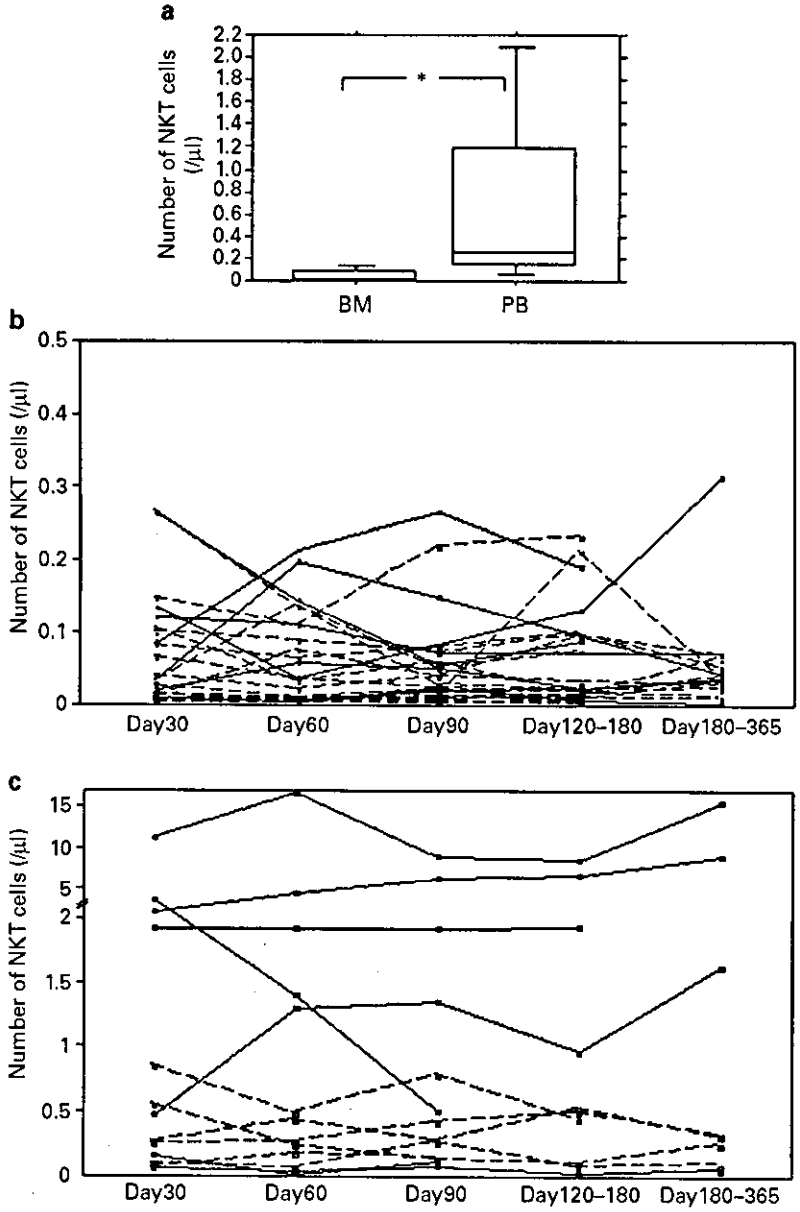

Figure 2 NKT cell recovery in BMT and PBSCT recipients. (a) Composite box plots for NKT on day 30 in BMT ($n=41$) and PBSCT ($n=18$). The number of NKT cells in patients who received PBSCT is significantly higher than that in patients who received BMT ($P<0.0001$). (b and c) NKT cell recovery in BMT (b) and PBSCT (c) patients. Lines show the individual recovery of NKT cells. Solid lines and closed circles show recovery in patients without GVHD. Dashed lines and open circles show recovery in patients with GVHD. We only show recovery in patients for whom blood samples could be obtained over four times (BMT) or over three times (PBSCT). The figure shows eight (BMT, without GVHD), 20 (BMT, with GVHD), seven (PBSCT, without GVHD), and six patients (PBSCT, with GVHD). The shaded gray area represents the 10–90th percentile values of normal controls.

patients than in other patients (Figure 4b). There were also fewer $CD4^-$ $V\alpha24^+$ NKT cells in chronic extensive GVHD patients, but this difference was not significant (Figure 4c). Again, the administration of steroids did not significantly affect the number of NKT cells (data not shown). Since the generation of murine $V\alpha14^+$ NKT cells is thought to be thymus dependent,[9] NKT cell reconstitution in humans may also be thymus dependent. However, the number of NKT cells did not correlate with the number of CD3 T cells (Figure 4d).

In PBSCT recipients, NKT cell counts in patients with GVHD were not significantly different than those in patients without GVHD (data not shown), although the number of NKT cells in patients without GVHD tended to be higher than that in patients with GVHD (Figure 2c).

As shown in Figure 2b, few GVHD patients with a normal NKT cell count on day 30 subsequently fell outside the normal range, and some patients showed the reverse trend (ie an abnormal NKT count became normal). Therefore, we examined NKT cell recovery and the timing of GVHD or other complications. Figure 5a shows NKT cell recovery in a 30-year-old male who received related BMT. He suffered from gut stage 3 acute GVHD. It was most severe on days 50 and 75, but subsided beginning on

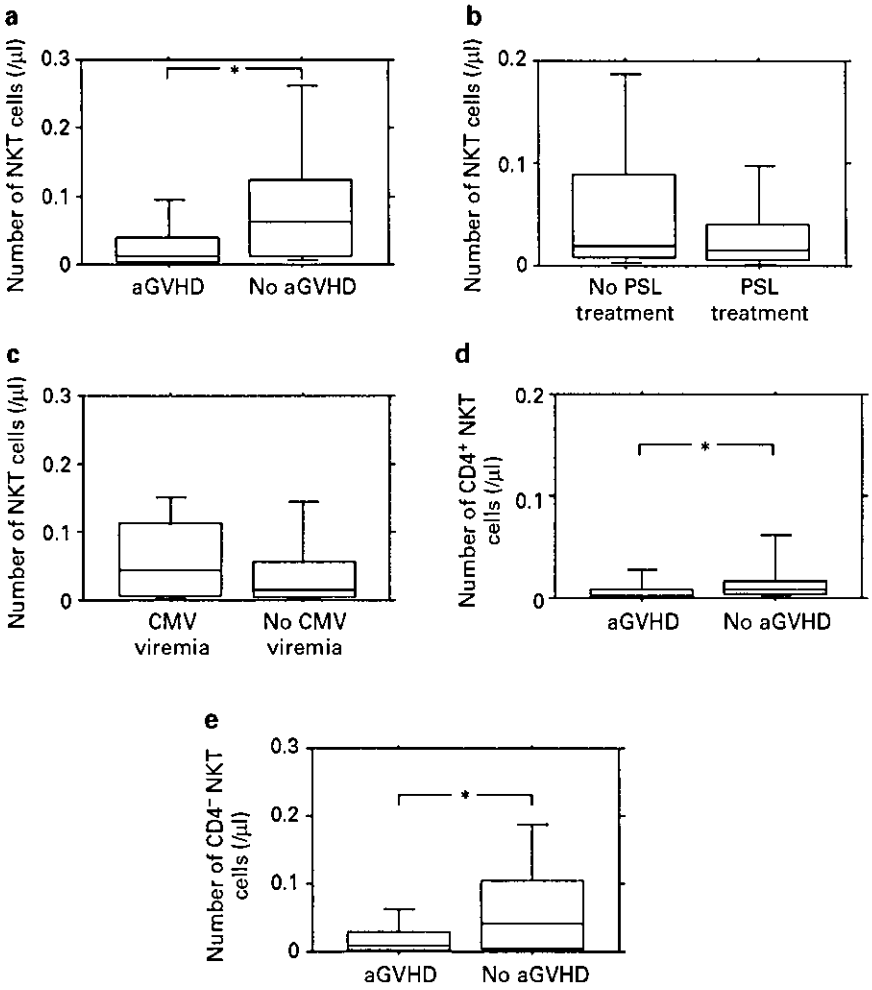

Figure 3 Number of Vα24+ NKT cells in BMT recipients with or without acute GVHD. (**a**) Composite box plots for NKT cells on day 30 in BMT recipients with ($n = 24$) or without ($n = 24$) acute GVHD The number of Vα24+ NKT cells in BMT recipients without acute GVHD was significantly higher than that in BMT recipients with acute GVHD ($P = 0.0172$). (**b**) Composite box plots for NKT cells on day 30 in BMT recipients with acute GVHD who did ($n = 22$) or did not ($n = 11$) receive steroid treatment. Steroid administration did not affect the number of NKT cells ($P = 0.4450$). (**c**) Composite box plots for NKT cells on day 60 in BMT recipients with ($n = 14$) or without ($n = 30$) CMV viremia. CMV viremia did not affect the number of NKT cells ($P = 0.2957$). (**d** and **e**) Composite box plots for CD4+ NKT (**d**) and CD4- NKT (**e**) cells on day 30 in BMT recipients with or without GVHD. Both CD4+ and CD4- Vα24+ NKT cells were significantly reduced in patients with acute GVHD (CD4+: $P = 0.0392$; CD4-: $P = 0.0337$). *$P < 0.05$. aGVHD, acute GVHD.

day 100. Figure 5b shows NKT cell recovery in a 34-year-old female who received unrelated BMT. She suffered from skin stage 3 GVHD on day 10. She received methylprednisolone pulse therapy and recovered quickly. She did not suffer from GVHD afterwards. Figure 5c shows NKT recovery in a 53-year-old female who received unrelated BMT. She suffered from skin stage 3 GVHD on day 17. Her GVHD responded to steroid treatment, but on day 100 she suffered from chronic lung GVHD. All of these cases suggest that GVHD may be correlated with a low number of NKT cells.

Discussion

In this study, we examined the recovery of Vα24+ NKT cells in patients who received hematopoietic stem cell transplantation and its correlation with GVHD. Many studies have suggested that an important physiological function of NKT cells is to control immune responses against infection and some tumors. In transplantation immunity, CD1d-dependent NKT cells are also thought to play a role in the induction of self[19] or allograft[20–22] or xenograft tolerance.[23] In a murine GVHD model, bone marrow DN NK1.1+ T cells were observed to be important for preventing GVHD.[10] Recently, NKT cells that were CD1d independent or that had diverse TCR-α chains have been reported. CD8+ CD1d-independent NKT cells have been shown to reduce GVHD.[11] Bone marrow noninvariant CD1d-restricted NKT cells that had the potential to suppress GVHD have been reported in humans.[17] However, to the best of our knowledge, there has been no previous report that human Vα24+ NKT cells prevented GVHD. In the present study, the number of Vα24+ NKT cells in BMT recipients with acute GVHD or chronic extensive GVHD was lower than that in recipients without

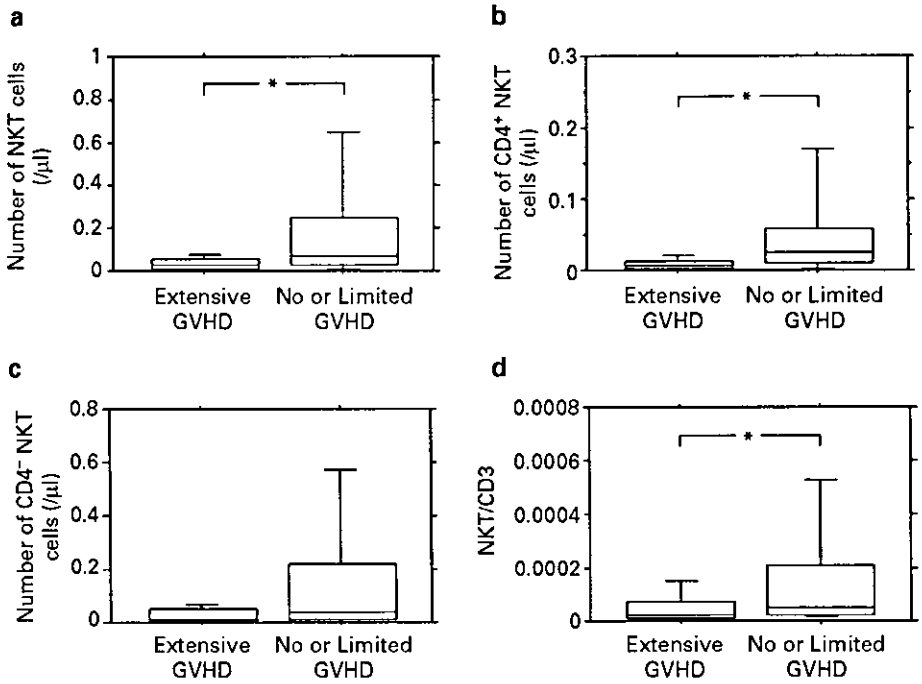

Figure 4 Number of Vα24+ NKT cells in BMT recipients with or without chronic GVHD. (**a**) Composite box plots for NKT in BMT recipients with chronic extensive GVHD ($n = 21$) or no or limited chronic GVHD ($n = 31$). The number of Vα24+ NKT cells in extensive GVHD patients was significantly lower than that in patients who had no or limited chronic GVHD ($P = 0.0089$). (**b** and **c**) Composite box plots for CD4+ Vα24+ (**b**) and CD4- Vα24+ (**c**) NKT cell counts in BMT recipients with extensive chronic GVHD or no or limited chronic GVHD. Chronic extensive GVHD patients had significantly fewer CD4+ and CD4- Vα24+ NKT cells than other patients. However, there was no significant difference in the CD4- Vα24+ NKT cell count (CD4+ NKT cells: $P = 0.0012$; CD4-NKT cells: $P = 0.0792$, respectively). (**d**) Composite box plots for the ratio of the NKT cell number to the CD3+CD56- T-cell number. The ratio is smaller in chronic extensive GVHD patients ($n = 16$) than in other patients ($n = 27$) ($P = 0.0148$). cGVHD, chronic GVHD.

GVHD. Thus, Vα24+ NKT cells may also function to suppress GVHD, although it is also possible that GVHD decreases the number of NKT cells. The administration of steroids, which is the most popular therapy for GVHD, did not suppress NKT cells. Moreover, the recovery of other lymphocytes (NK cells, B cells, CD4+ T cells, CD8+ T cells, CD4+CD45RA+ T cells, and CD4+CD45RO+ T cells) was not significantly affected by the presence of acute or chronic GVHD (data not shown). Therefore, the low number of NKT cells in patients with GVHD did not result from a delay in lymphocyte recovery. Further analyses using animal models are needed to determine whether the reduced number of NKT cells is a cause or an effect of GVHD.

NKT cells consist of three subsets: DN, CD4+, and CD8+ cells. CD4+ NKT cells produce large amounts of IL-4, while CD4- (DN and CD8+) NKT cells selectively produce Th1 cytokines.[14,15,24] The numbers of both CD4+ and CD4- NKT cells were reduced in acute GVHD patients. It has been suggested that the Th1/Th2 balance influences the development of acute GVHD. For example, there are some reports that Th1 cells cause acute GVHD more efficiently than Th2 cells, and that Th2 cells suppress GVHD.[25-27] Other data have suggested that Th1 cytokines reduced acute GVHD or that Th2 cytokines worsened acute GVHD.[28-30] In any case, it may be important to regulate both Th1 and Th2 cytokines to control GVHD, and thus CD4+ and CD4- Vα24+ NKT cells likely play some roles in preventing acute GVHD.

In the case of chronic GVHD, there were significantly fewer CD4+ Vα24+ NKT cells in patients with chronic extensive GVHD than in those with no or limited GVHD. There also tended to be fewer CD4- Vα24+ NKT cells in chronic extensive GVHD patients, although this difference was not significant. In some reports, Th2 cytokines have been recognized as the principal mediators of chronic GVHD.[19,26] The protective effect against GVHD was strictly dependent on IL-4 production from NKT cells.[10,31] Moreover, CD4+ Vα24+ NKT cells produce large amounts of IL-10,[25,32] and NKT cell-derived IL-10 was essential for the differentiation of antigen-specific regulatory T cells in systemic tolerance.[33] Thus, CD4+ NKT cells that produce Th2 cytokines may suppress the Th1 response and control GVHD.

Recent reports have shown that CD4+CD25+ T cells suppress GVHD.[34] CD4+CD25+ T cells are known to be immune regulatory cells and are essential for the induction and maintenance of self-tolerance and for the protection of autoimmunity. We failed to show that the number of CD4+CD25+ T cells correlated with GVHD (data not shown). CD25 is also expressed when CD4+ T cells are activated in GVHD. Therefore, it might be difficult to count only suppressor T cells.

In Japan, PBSCT is only available to patients who have a related donor, and thus BMT is performed for patients with an unrelated donor. On the other hand, many related hematopoietic stem cell transplantations are PBSCT (we think that this is why the incidence of relapse in the PBSCT

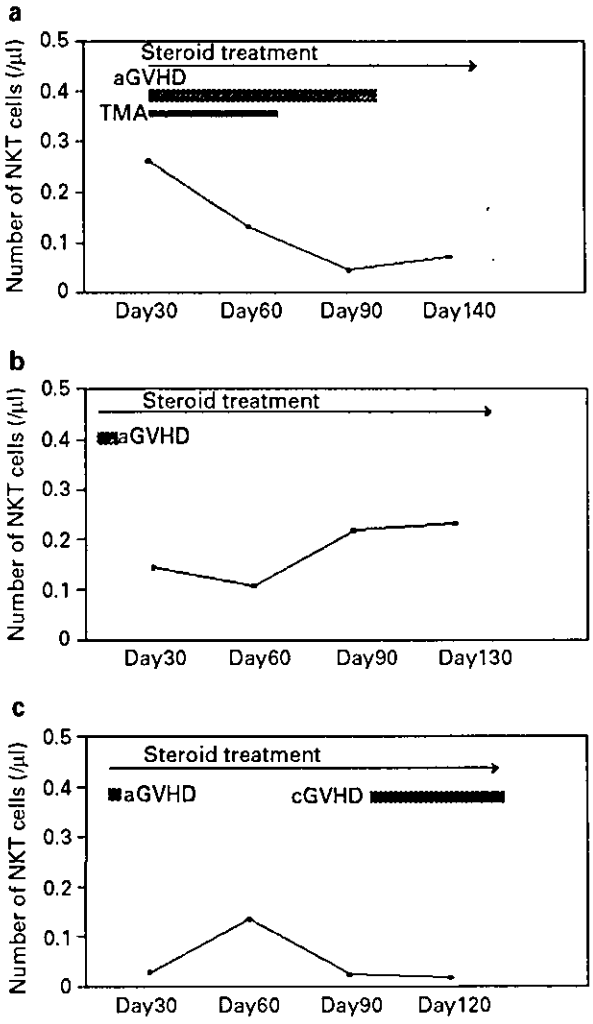

Figure 5 NKT cell recovery and the clinical course in three BMT recipients. (**a**) A 30-year-old male who received related BMT. (**b**) A 34-year-old female who received unrelated BMT. (**c**) A 53-year-old female who received unrelated BMT. Details are provided in the text.

group was higher than that in BMT recipients). Therefore, we cannot simply compare the reconstitution of NKT cells between PBSCT and BMT. However, the difference is so significant that we could safely conclude that the recovery of NKT cells in patients who received PBSCT is much faster than that in patients who received BMT. One possible reason is that PBSC grafts contain more NKT cells than BM grafts. A previous report showed that the number of Vα24+ invariant NKT cells in BM was comparable to or less than that in peripheral blood mononuclear cells.[17] These findings indicate that PBSC grafts contain many more Vα24+ NKT cells than BM grafts. Chimerism of invariant NKT cells in the chronic phase was donor type, but it is difficult to investigate chimerism in the early phase, especially after BMT because there are extremely few invariant NKT cells. In PBSCT, we failed to show that there were significantly fewer NKT cells in patients with GVHD. One possible reason is that there were very few patients in this study and another is that the number of NKT cells varied widely among individuals.

In conclusion, Vα24+ NKT cells were reconstituted rapidly in PBSCT recipients and slowly in BMT recipients. The number of Vα24+ NKT cells in patients with GVHD was lower than that in patients without GVHD, and the number of CD4+ NKT cells in GVHD patients is especially low. Our results raise the possibility that the therapeutic administration of Vα24+ NKT cells or α-galactosylceramide might ameliorate GVHD. Thus, NKT cells should be considered as an exciting new modality of cellular therapy for the regulation of undesirable immune responses.

Acknowledgements

We thank Eri Nagata for providing excellent technical assistance.

References

1 Fujimaki K, Maruta A, Yoshida M *et al.* Immune reconstitution assessed during five years after allogeneic bone marrow transplantation. *Bone Marrow Transplant* 2001; **27**: 1275–1281.
2 Storek J, Dawson MA, Storer B *et al.* Immune reconstitution after allogeneic marrow transplantation compared with blood stem cell transplantation. *Blood* 2001; **97**: 3380–3389.
3 Fowlkes BJ, Kruisbeek AM, Ton-That H *et al.* A novel population of T cell receptor αβ-bearing thymocytes which predominantly express a single Vβ8 gene family. *Nature* 1987; **329**: 251–254.
4 Budd RC, Miescher GC, Howe RC *et al.* Developmentally regulated expression of T cell receptor β chain variable domain is immature thymocytes. *J Exp Med* 1987; **166**: 577–582.
5 Lantz O, Bendelac A. An invariant T cell receptor α chain is used by a unique subset MHC class I-specific CD4+ and CD4−CD8−T cells in mice and humans. *J Exp Med* 1994; **180**: 1097–1106.
6 Dellabona P, Padovan E, Casorati G *et al.* An invariant Vα-JαQ/Vα11 T cell receptor is expressed in all individuals by clonally expanded CD4−CD8− cells. *J Exp Med* 1994; **180**: 1171–1176.
7 Porcelli S, Gerdes D, Fertig AM, Balk SP. Human T cells expressing an invariant Vα24-JαQ TCRα are CD4− and heterogeneous with respect to TCRβ expression. *Hum Immunol* 1996; **48**: 63–67.
8 Godfrey DI, Hammond KJL, Poulton LD, Baxter AG. NKT cells: facts, functions and fallacies. *Immunol Today* 2000; **21**: 573–583.
9 Joyce S. CD1d and natural T cells: how their properties jump-start the immune system. *Cell Mol Life Sci* 2001; **58**: 442–469.
10 Zeng D, Lewis D, Dejbakhsh-Jones S *et al.* Bone marrow NK1.1− and NK1.1+ T cells reciprocally regulate acute graft versus host disease. *J Exp Med* 1999; **189**: 1073–1081.
11 Baker J, Verneris MR, Ito M *et al.* Expansion of cytolytic CD8+ natural killer T cells with limited capacity for graft-versus-host disease induction due to interferon γ production. *Blood* 2001; **97**: 2923–2931.
12 Thiede C, Florek M, Bornhäuser M *et al.* Rapid quantification of mixed chimerism using multiplex amplification of short tandem repeat markers and fluorescence detection. *Bone Marrow Transplant* 1999; **23**: 1055–1060.
13 Takahashi T, Nieda M, Koezuka Y *et al.* Analysis of human Vα24+CD4+ NKT cells activated by α-galactosylceramide-

pulsed monocyte-derived dendritic cells. *J Immunol* 2000; **164**: 4458–4464.
14 Takahashi T, Chiba S, Nieda M *et al.* Analysis of human Vα24+CD8+ NKT Cells activated by α-galactosylceramide-pulsed monocyte-derived dendritic cells. *J Immunol* 2002; **168**: 3140–3144.
15 Karadimitris A, Gadola S, Altamirano M *et al.* Human CD1d-glycolipid tetramers generated by *in vitro* oxidative refolding chromatography. *Proc Natl Acad Sci USA* 2001; **98**: 3294–3298.
16 Lee PT, Benlagha K, Teyton L, Bendelac A. Distinct functional lineages of human Vα24 natural killer T cells. *J Exp Med* 2002; **195**: 637–641.
17 Exley MA, Tahir SMA, Cheng O *et al.* A major fraction of human bone marrow lymphocyte are Th2-like CD1d-reactive T cells that can suppress mixed lymphocyte responses. *J Immunol* 2001; **167**: 5531–5534.
18 Kim CH, Johnston B, Butcher EC. Trafficking machinery of NKT cells: shared and differential chemokine receptor expression among Vα24+Vβ11+ NKT cell subsets with distinct cytokine-producing capacity. *Blood* 2002; **100**: 11–16.
19 Sonoda K, Exley M, Snapper S *et al.* CD1-reactive natural killer T cells are required for development of systemic tolerance through an immune-privileged site. *J Exp Med* 1999; **190**: 1215–1225.
20 Seino K, Fukao K, Muramoto K *et al.* Requirement for natural killer T (NKT) cells in the induction of allograft tolerance. *Proc Natl Acad Sci USA* 2001; **98**: 2577–2581.
21 Chargui J, Hase T, Wada S *et al.* NKT cells as nonspecific immune-regulator inducing tolerance in mouse model transplantation. *Transplant Proc* 2001; **33**: 3833–3834.
22 Higuchi M, Zeng D, Shizuru J *et al.* Immune tolerance to combined organ and bone marrow transplants after fractionated lymphoid irradiation involves regulatory NKT cells and clonal deletion. *J Immunol* 2002; **169**: 5564–5570.
23 Ikehara Y, Yasunami Y, Kodama S *et al.* CD4+Vα24 natural killer T cells are essential for acceptance of rat islet xenografts in mice. *J Clin Invest* 2000; **105**: 1761–1767.
24 Gumperz JE, Miyake S, Yamamura T, Brenner MB. Functionally distinct subsets of CD1d-restricted natural killer T cells revealed by CD1d tetramer staining. *J Exp Med* 2002; **195**: 625–636.
25 Teshima T, Ferrara JLM. Understanding the alloresponse: new approaches to graft-versus-host disease prevention. *Semin Hematol* 2002; **39**: 15–22.
26 Ellison CA, Fischer JMM, HayGlass KT, Gartner JG. Murine graft-versus-host disease in an F1-hybrid model using IFN-α gene knockout donors. *J Immunol* 1998; **161**: 631–640.
27 Allen RD, Staley TA, Sidman CL. Differential cytokine expression in acute and chronic murine graft-versus-host-disease. *Eur J Immunol* 1993; **23**: 333–337.
28 Brok HPM, Heidt PJ, van der Meide PH *et al.* Interferon-γ prevents graft-versus-host disease after allogeneic bone marrow transplantation in mice. *J Immunol* 1993; **151**: 6451–6459.
29 Yang YG, Dey BR, Sergio JJ *et al.* Donor-derived interferon γ is required for inhibition of acute graft-versus-host disease by interleukin 12. *J Clin Invest* 1998; **102**: 2126–2135.
30 Murphy WJ, Welniak LA, Taub DD *et al.* Differential effects of the absence of interferon-γ and IL-4 in acute graft-versus-host disease after allogeneic bone marrow transplantation in mice. *J Clin Invest* 1998; **102**: 1742–1748.
31 Lan F, Zeng D, Higuchi M *et al.* Predominance of NK1.1+TCRαβ+ or DX5+TCRαβ+ T cells in mice conditioned with fractionated lymphoid irradiation protects against graft-versus-host disease: 'natural suppressor' cells. *J Immunol* 2001; **167**: 2087–2096.
32 Takahashi T, Nakamura K, Chiba S *et al.* Vα24+ natural killer T cells are markedly decreased in atopic dermatitis patients. *Hum Immunol* 2003; **64**: 586–592.
33 Sonoda K, Faunce DE, Taniguchi M *et al.* NK T cell-derived IL-10 is essential for the differentiation of antigen-specific T regulatory cells in systemic tolerance. *J Immunol* 2001; **166**: 42–50.
34 Taylor PA, Lees CJ, Blazar BR. The infusion of *ex vivo* activated and expanded CD4+CD25+ immune regulatory cells inhibits graft-versus-host disease lethality. *Blood* 2002; **99**: 3493–3499.

The transcriptionally active form of AML1 is required for hematopoietic rescue of the *AML1*-deficient embryonic para-aortic splanchnopleural (P-Sp) region

Susumu Goyama, Yuko Yamaguchi, Yoichi Imai, Masahito Kawazu, Masahiro Nakagawa, Takashi Asai, Keiki Kumano, Kinuko Mitani, Seishi Ogawa, Shigeru Chiba, Mineo Kurokawa, and Hisamaru Hirai

Acute myelogenous leukemia 1 (AML1; runt-related transcription factor 1 [Runx1]) is a member of Runx transcription factors and is essential for definitive hematopoiesis. Although AML1 possesses several subdomains of defined biochemical functions, the physiologic relevance of each subdomain to hematopoietic development has been poorly understood. Recently, the consequence of carboxy-terminal truncation in AML1 was analyzed by the hematopoietic rescue assay of *AML1*-deficient mouse embryonic stem cells using the gene knock-in approach. Nonetheless, a role for specific internal domains, as well as for mutations found in a human disease, of AML1 remains to be elucidated. In this study, we established an experimental system to efficiently evaluate the hematopoietic potential of AML1 using a coculture system of the murine embryonic para-aortic splanchnopleural (P-Sp) region with a stromal cell line, OP9. In this system, the hematopoietic defect of *AML1*-deficient P-Sp can be rescued by expressing AML1 with retroviral infection. By analysis of AML1 mutants, we demonstrated that the hematopoietic potential of AML1 was closely related to its transcriptional activity. Furthermore, we showed that other Runx transcription factors, Runx2/AML3 or Runx3/AML2, could rescue the hematopoietic defect of *AML1*-deficient P-Sp. Thus, this experimental system will become a valuable tool to analyze the physiologic function and domain contribution of Runx proteins in hematopoiesis. (Blood. 2004;104:3558-3564)

© 2004 by The American Society of Hematology

Introduction

Acute myelogenous leukemia 1 (AML1)/runt-related transcription factor 1 (Runx1) belongs to a family of transcriptional regulators called Runx, which contain a conserved 128–amino acid Runt domain responsible for sequence-specific DNA binding.[1] Runx proteins make heterodimeric complexes with a partner protein, CBFβ/PEBP2β (core-binding factor β/polyomavirus enhancer–binding protein 2β),[2-4] and this association is essential for its biologic activity.[5-7] There are 3 known mammalian Runx family members: AML1/Runx1, Runx2/AML3, and Runx3/AML2. Typically, Runx functions as a transcriptional activator of target gene expression. Under some conditions, however, it can repress the transcription of specific genes.

AML1 was originally identified on chromosome 21 as the gene that is disrupted in the (8;21)(q22;q22) translocation, which is one of the most frequent chromosome abnormalities associated with human AML.[8,9] Subsequently, AML1 was shown to be one of the most frequent targets of leukemia-associated gene aberrations.[10,11] Moreover, somatic point mutations of the *AML1* gene were also demonstrated in patients with AML and myelodysplastic syndrome (MDS).[12-14] In addition to a role in leukemic transformation, gene-targeting studies in mice have demonstrated that AML1 is essential for early development of definitive hematopoiesis. *AML1*-deficient embryos develop through the yolk sac stage but die around 12 to 13 days of gestation following complete block of fetal liver hematopoiesis.[15,16]

AML1 includes at least 3 alternative splicing forms: AML1a, AML1b, and AML1c.[17] In AML1b and AML1c, the carboxy (C)–terminal to the Runt domain lies in a region that contains sequences of defined biochemical functions, which are absent in AML1a. Several functional domains have been identified in the C-terminal half, such as *trans*-activation domain,[18,19] *trans*-repression domain,[20] and VWRPY motif.[21-23]

During vertebrate embryogenesis, hematopoietic development consists of 2 distinct waves of discrete cellular components known as primitive and definitive hematopoiesis.[24] In mice, the first wave of primitive hematopoiesis, which consists predominantly of a large and nucleated erythroid cell, emerges in the yolk sac at 7.5 embryonic days after coitus (dpc). Then, primitive hematopoiesis begins to be replaced around 9.5 dpc by definitive hematopoiesis, generally described as the second wave. Progenitors for definitive hematopoiesis originate from para-aortic splanchnopleural (P-Sp) region at 7.5 to 9.5 dpc,[25,26] and long-term repopulating hematopoietic stem cells (LTR-HSCs) that can reconstitute adult mice appear in the aorta-gonad-mesonephros (AGM) at 10.5 to 11.5 dpc.[27,28] These cells subsequently colonize the fetal liver, where they expand and differentiate. Active sites for definitive hematopoiesis

From the Departments of Hematology/Oncology and Regeneration Medicine for Hematopoiesis, Graduate School of Medicine, University of Tokyo, Tokyo, Japan; Department of Cell Therapy/Transplantation Medicine, University of Tokyo Hospital, University of Tokyo, Tokyo, Japan; and Department of Hematology, Dokkyo University School of Medicine, Tochigi, Japan.

Submitted April 22, 2004; accepted July 6, 2004. Prepublished online as *Blood* First Edition Paper, July 22, 2004; DOI 10.1182/blood-2004-04-1535.

Supported in part by a Grant-in-Aid for Scientific Research from the Japan Society for the Promotion of Science and by Health and Labour Sciences Research grants from the Ministry of Health, Labour, and Welfare.

An Inside *Blood* analysis of this article appears in the front of this issue.

Reprints: Mineo Kurokawa, Department of Hematology & Oncology, Graduate School of Medicine, University of Tokyo, 7-3-1 Hongo, Bunkyo-ku, Tokyo 113-8655, Japan; e-mail: kurokawa-tky@umin.ac.jp.

The publication costs of this article were defrayed in part by page charge payment. Therefore, and solely to indicate this fact, this article is hereby marked "advertisement" in accordance with 18 U.S.C. section 1734.

© 2004 by The American Society of Hematology